Journal of Medicinal Chemistry

ARTICLE

pubs.acs.org/jmc

Lead Optimization of Aryl and Aralkyl Amine-Based Triazolopyrimidine Inhibitors of *Plasmodium falciparum* Dihydroorotate Dehydrogenase with Antimalarial Activity in Mice

Ramesh Gujjar,[†] Farah El Mazouni,[§] Karen L. White,[∥] John White,[†] Sharon Creason,[‡] David M. Shackleford,[∥] Xiaoyi Deng,[§] William N. Charman,[∥] Ian Bathurst,[⊥] Jeremy Burrows,[⊥] David M. Floyd,[⊥] David Matthews,[⊥] Frederick S. Buckner,[‡] Susan A. Charman,[∥] Margaret A. Phillips,*[,§] and Pradipsinh K. Rathod*[,†]

[†]Departments of Chemistry and Global Health and [‡]Medicine, University of Washington, Seattle, Washington 98195, United States

[§]Department of Pharmacology, University of Texas Southwestern Medical Center at Dallas, 6001 Forest Park Boulevard, Dallas, Texas 75390-9041, United States

[∥]Centre for Drug Candidate Optimisation, Monash Institute of Pharmaceutical Sciences, Monash University (Parkville Campus), Parkville, VIC 3052, Australia

[⊥]Medicines for Malaria Venture, Geneva, Switzerland

ABSTRACT: Malaria is one of the leading causes of severe infectious disease worldwide; yet, our ability to maintain effective therapy to combat the illness is continually challenged by the emergence of drug resistance. We previously reported identification of a new class of triazolopyrimidine-based *Plasmodium falciparum* dihydroorotate dehydrogenase (*Pf*DHODH) inhibitors with antimalarial activity, leading to the discovery of a new lead series and novel target for drug development. Active compounds from the series contained a triazolopyrimidine ring attached to an aromatic group through a bridging nitrogen atom. Herein, we describe systematic efforts to optimize the aromatic functionality with the goal of improving potency and in vivo properties of compounds from the series. These studies led to the identification of two new substituted aniline moieties (4-SF_5-Ph and 3,5-Di-F-4-CF_3-Ph), which, when coupled to the triazolopyrimidine ring, showed good plasma exposure and better efficacy in the *Plasmodium berghei* mouse model of the disease than previously reported compounds from the series.

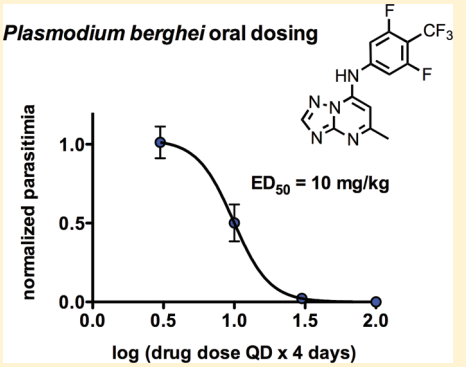

INTRODUCTION

Malaria remains one of the most significant infectious diseases worldwide. It is endemic in over 90 countries and leads to the death of 1−2 million people yearly, with a high prevalence of severe disease in children and pregnant woman.[1,2] The goal of eventual worldwide malaria eradication is now widely recognized. The approval of artemisinin-based combination therapies (ACTs) has led to substantial reductions in the burden of the disease, and these drugs are a key component of the eradication ambitions.[3] Past efforts to eliminate malaria have ended in the face of widespread drug resistance to the available agents.[4,5] In a worrying development, decreased artemesinin effectiveness has recently been found along the Cambodia−Thailand border, raising the concern that the value of ACTs will be increasingly compromised.[6,7] The challenge for the future is to find successful strategies to overcome the parasites' unwavering ability to circumvent drug therapies through resistance. This goal depends on a continuing pipeline of new antimalarials, as effective vaccines have not yet been identified.[8,9]

Pyrimidine metabolism has proven to be a vulnerable component of the malaria parasite's biology and is the target of a significant number of the clinically effective therapies, including pyrimethamine and other dihydrofolate reductase inhibitors, and atovaquone, an inhibitor of the bc1 complex.[1,10] The malaria parasite relies on the de novo pyrimidine biosynthetic pathway to obtain pyrimidine nucleotides, and unlike the host, it cannot salvage preformed pyrimidine bases or nucleosides.[11] This vulnerability has led to a significant focus on identifying new targets within the pyrimidine biosynthetic pathway. Efforts to target the fourth enzyme in the de novo biosynthetic pathway, dihydroorotate dehydrogenase (DHODH), are the most advanced.

DHODH catalyzes the flavin mononucleotide (FMN)-dependent oxidation of dihydroorotate to generate orotic acid.[11] The enzyme from different species can be divided into two classes, those that are cytoplasmic and utilize fumarate or nicotinamide adenine dinucleotide (NADH) to oxidize the FMN cofactor (class 1) or those that are localized in the mitochondria and utilize ubiquinone (coenzyme Q; CoQ) as the final oxidant (class 2). Both malarial and human DHODHs are class 2 mitochondrial enzymes. Potent and species selective inhibitors of *Plasmodium falciparum* dihydroorotate dehydrogenase (*Pf*DHODH), which

Received: March 7, 2011
Published: April 25, 2011

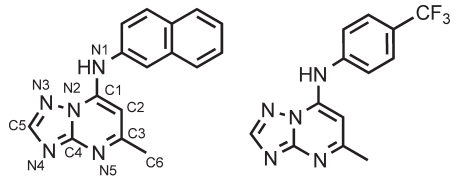

1 2

Figure 1. Structures of triazolopyrimidine *Pf*DHODH inhibitors **1** and **2**.

Scheme 1. Synthesis of the Triazolopyrimidine Compounds 7−52, 55−61[a]

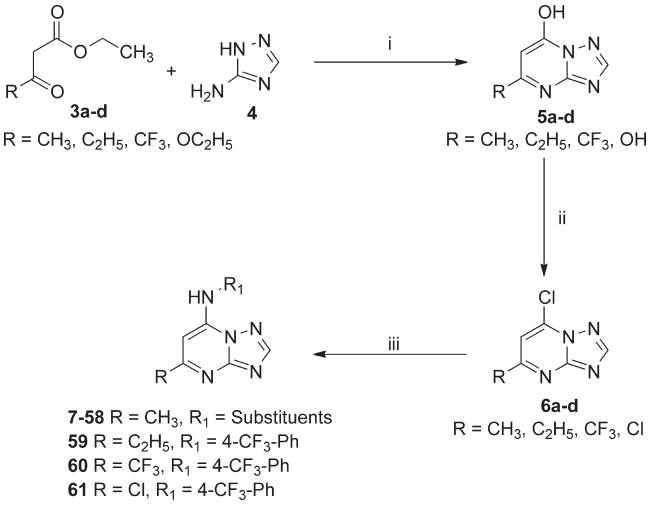

[a] Reagents and conditions: (i) AcOH, 3.5−8 h, reflux, 45−55% (**5a**−**c**)/NaOEt, EtOH, 8 h, 50% (**5d**); (ii) $POCl_3$, 30−45 min, reflux, 50−65% (**6a**−**c**)/$POCl_3$, DMA, 1.5 hr, reflux, 68% (**6d**); (iii) R_1−NH_2, EtOH/DMF-K_2CO_3, 2−20 h, rt, 50−92%.

are inactive against the human enzyme and which showed good activity against the parasites in whole cell assays, have been identified by high-throughput screening (HTS).[12−14] From these efforts, two series have emerged as viable leads for the development of a new antimalarial agent targeting DHODH: the triazolopyrimidines identified by our group (Figure 1)[13,15] and the thiophenecarboxamides identified by Genzyme and collaborators.[14,16] Both series are currently undergoing lead optimization programs, and these efforts have led to the identification of compounds with some activity against the malaria parasite in mouse models.[15,16] The structural basis for the species selectivity of these lead inhibitors has been demonstrated by X-ray structure determination of compounds from both series in complex with *Pf*DHODH.[16,17] These studies have identified a number of differences in amino acid composition between the human and malarial enzyme in the inhibitor binding pockets that account for the species selectivity of the series.

The initial lead compound **1** {5-methyl-[1,2,4]triazolo[1,5-*a*]-pyrimidin-7-yl)-naphthalen-2-yl-amine (DSM1)} in the triazolopyrimidine series showed good activity against both the enzyme and the parasite (IC_{50} values in the range of 50−100 nM) but showed poor plasma exposure after repeat dosing.[15] Subsequent medicinal chemistry efforts identified a metabolically stable compound **2** [5-methyl-[1,2,4]triazolo[1,5-*a*]pyrimidin-7-yl)-(4-trifluoromethyl-phenyl)-amine (DSM74)] that was able to suppress parasite growth in the *P. berghei* mouse model of the disease, providing the first proof of concept that *Pf*DHODH inhibitors could have antimalarial activity in vivo.[15] However, while compound **2** showed improved plasma exposure, it was less potent than the original lead compound **1** as assessed in assays against *Pf*DHODH and *P. falciparum* in culture. Our goal here was to identify a novel set of triazolopyrimidines with improved potency and prolonged plasma exposure, with the assumption that this would lead to improved in vivo efficacy against the malaria parasite in mouse models of malaria.

CHEMISTRY

Compounds **7**−**52** and **55**−**61** were synthesized as shown in Scheme 1 using previously described methods.[13,15,18] Briefly, condensation of 3-amino-[1,2,4]triazole **4** with substituted ethyl acetoacetate **3a**−**c** in acetic acid or with diethyl malonate **3d** in NaOEt in EtOH gave the substituted 7-hydroxy-[1,2,4]triazolo-[1,5-*a*]pyrimidine **5a**−**c**/5,7-dihydroxy-[1,2,4]triazolo[1,5-*a*]pyrimidine **5d**. Chlorination with $POCl_3$ gave the corresponding 7-chloro-[1,2,4]triazolo[1,5-*a*]pyrimidine **6a**−**c**/5,7-dichloro-[1,2,4]-triazolo[1,5-*a*]pyrimidine **6d**, which upon treatment with substituted amines in ethanol/DMF-K_2CO_3 resulted in the desired products **7**−**52** and **55**−**61**.

For compounds **26** and **27**, it was necessary to synthesize the corresponding aryl amine precursors **69** and **70** (scheme 2). The aryl amines **69** and **70** were prepared using 1-fluoro-4-nitrobenzene **66** by aromatic nucleophilic substitution with *tert*-butyl amine/potassium *tert*-butoxide to provide nitro compounds **67** and **68**. The nitro groups were then reduced with hydrogen in the presence of Pd/C catalyst to their corresponding amino compounds **69** and **70**.

RESULTS

Systematic Substitution of the Aryl Amine Moiety. Previously identified triazolopyrimidines in the series showed either poor metabolic stability leading to poor plasma exposure or lacked potency, so we undertook an extensive search for aryl amine replacements that would improve potency while maintaining good plasma exposure after oral dosing. The X-ray structure of **1** and **2** bound to *Pf*DHODH demonstrated that the binding pocket for the aryl amine is completely hydrophobic and unable to form any H-bonding interactions (Figure 2).[17] The structures also showed that the pocket between the aryl amine (N1) (Figure 1) and the aromatic ring binding site is narrow, seemingly consistent with the observation that *ortho* substituents on the aniline ring are not tolerated.[15] Therefore, no additional compounds of this type were synthesized. However, structural data from several analogues with differing aromatic ring systems and substitutions indicated significant conformational flexibility in the hydrophobic pocket accommodating the aromatic ring, which supported further investigation of the effects of modifications in this region of the inhibitor molecule. To this end, we identified a series of amines (mostly commercially available) and coupled these to the triazolopyrimidine scaffold using the procedures established for the synthesis of **1** and **2** (Experimental Section) (Scheme 1). These analogues were designed to further explore binding requirements in this region of the enzyme.

All of the new compounds were analyzed for their ability to inhibit *Pf*DHODH, and select compounds were evaluated against the human and *P. berghei* enzymes to explore species selectivity (Table 1). Compounds were also evaluated for efficacy

Scheme 2. Synthesis of Aryl Amine Precursors 69 and 70[a]

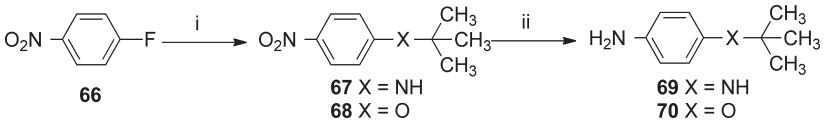

[a] Reagents and conditions: (i) *t*-Bu-NH_2, DMSO, 96 h, 50 °C, 77% (**67**)/*t*-BuOK, DMF, 2 h, 56% (**68**). (ii) Pd-C, H_2, 3−10 h, room temperature, 80−85%.

against *P. falciparum* 3D7 cells in vitro. A good correlation between *Pf*DHODH inhibitor activity and inhibition of *P. falciparum* 3D7 cell growth were observed throughout the series (Figure 3). The most potent analogs in the series were highly hydrophobic and similar in size to the naphthyl moiety of **1**. These compounds include **15** (*para*-tert butyl-Ph), **29** (*para*-*tert*-butyl-Ph, *meta*-fluorine), **33** (5,6,7,8-tetrahydro-2-naphthyl), and **36** (5-benzothiophenyl). All four compounds showed similar potency to **1** against *Pf*DHODH (IC_{50} < 100 nM) and *P. falciparum* 3D7 cells (EC_{50} = 50−150 nM), while retaining selectivity against the human enzyme. Notably, two of these compounds, **33** and **36**, are naphthyl analogues. The replacement of 5,6,7,8-tetrahydro-2-naphthyl **33** with the similar but smaller 5-indanyl **34** reduced activity (IC_{50} = 0.035 vs 0.22 μM, respectively), suggesting that subtle differences in size or shape appear to have a significant impact on binding and, hence, potency in this series. Unlike **36** where the addition of sulfur into the aromatic ring system was favorable, the addition of nitrogen (**37**) or oxygen (**35**) was highly unfavorable, consistent with the hydrophobic nature in this area of the binding site (Figure 2).

Aliphatic substitution at the *para* position on the aniline moiety was explored with respect to potency against the *Pf*DHODH enzyme (**7**−**18**). Consistent with the hydrophobic nature of this binding interaction, the *tert*-butyl analogue **15** was the most potent. The branched chain *iso*-propyl analogue **14**,[19] the straight chain analogues (**7**−**10**), and the unsaturated analogues **17** and **18** were somewhat less potent. Also consistent with our structural data, as the chain size increased beyond five carbons, the potency decreased apparently associated with the fact that the binding site could no longer accommodate the increase in size. In fact, the apparent penalty in binding affinity increased with increasing chain length from *n*-pentyl to *n*-octyl (**10**−**13**). The activity of cyclopropyl analogue **16** was similar to *n*-propyl analogue **8** and the isopropyl analogue **14**. The substitution of larger five- and six-membered rings containing heteroatoms at the *para* position was strongly disfavored (**24** and **25**) as was the addition of an N or O linker to the *tert*-butyl group (**26** and **27**), further suggesting significant steric constraints in this area of the enzyme binding pocket. An additional demonstration that hydrophilic/polar functionality is not tolerated is evidenced by the lower potency of the 4-$N(CH_3)_2$ analogue **23**, which is similar in size to *iso*-propyl **14** but 4-fold less potent on *Pf*DHODH. The substitution of CN for a methyl in the *tert*-butyl structure (**28** vs **15**) leads to a 13-fold reduction in inhibitory activity, again possibly due to the introduction of polar functionality.

Next, we evaluated a set of fluorinated groups at the *para* and *meta* positions of the aniline group. The substitution of 4-SF_5 for 4-CF_3 resulted in a compound **21** with 2−3-fold better activity against *Pf*DHODH than **2** (Table 1), possibly due to the increase in hydrophobicity with SF_5 as compared to CF_3. However, the addition of a second CF_3 group onto the ring at the *meta* position in **31** (3,4-di-CF_3-Ph) led to a decrease in potency relative to **2**. The addition of a sulfur linker between the phenyl and the CF_3 (**20**) reduced activity by several fold versus **2**, while the addition

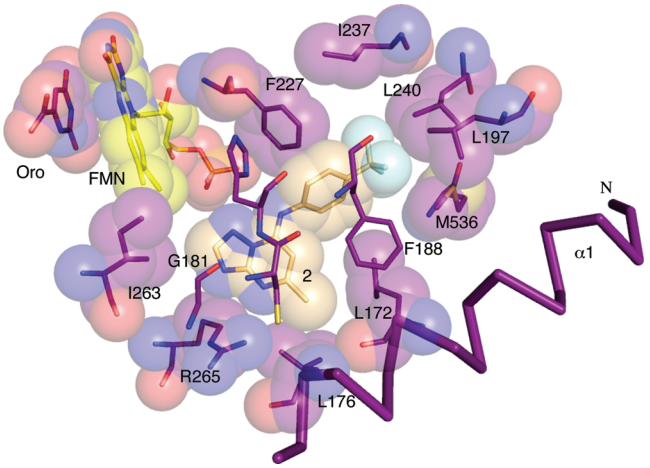

Figure 2. Inhibitor binding site of **2** bound to *Pf*DHODH. The pdb file 3I6R was used to generate the figure.[17] A limited set of residues within the 4 Å shell of **2** are displayed (residues behind **2** were removed for clarity). Residues and ligands are shown as space-filling balls, with the exception of residues in the front of **2**, where they are shown as sticks for clarity. Amino acid residues and orotate (Oro) are colored purple, FMN in yellow, and **2** in tan. Nitrogen, blue; oxygen, red; sulfur, yellow; and fluorine, light blue. The figure is displayed using PyMol (DeLano, W. L. The PyMOL Molecular Graphics System, 2002; http://www.pymol.org).

of a methyl linker (**19**) reduced activity by nearly 10-fold. Both of these results are consistent with the observed size constraints in this area of the molecule. The addition of a *meta*-fluorine to the aniline ring was tested in combination with some of the better *para* substituents (CF_3 or *tert*-butyl) and provided somewhat improved potency in each case (2-fold decreases in *Pf*DHODH IC_{50} were observed for **2** vs **32** and **15** vs **29**). We previously reported the activity of the 4-Cl-Ph aryl substituent (DSM89[15]). In comparison, the addition of the *meta*-fluorine **30** to 4-Cl-Ph decreases the *Pf*DHODH IC_{50} by 3-fold over the 4-Cl alone.

The EC_{50} for **21** and **32** against the parasite in our standard whole cell assay that utilizes serum was 10-fold higher than the activity observed on the enzyme (Table 1). However, when these compounds were retested using Albumax as a replacement for serum, the EC_{50} for inhibition of 3D7 growth decreased and became similar to the enzyme inhibition data (EC_{50} = 0.18 and 0.22 μM, respectively). In contrast, the activity of **1** was similar in the two media. Previous studies have suggested that protein binding can influence how compounds behave under these different assay conditions,[20] providing a possible explanation as to why compounds **21** and **32** perform differently in the two media.

Nonaromatic Substitutions and Addition of Linkers between the Aniline and the Triazolopyrimidine. A series of nonaromatic cyclic and linear alkyl substitutions were also explored as aryl amine replacements (Table 2). The nonaromatic cyclic compounds **38**−**44** ranged in ring size from 3 to 12 carbons.

dx.doi.org/10.1021/jm200265b |*J. Med. Chem.* 2011, 54, 3935–3949

Table 1. SAR of Substituted Aryl Amine-Based Triazolopyrimidine Derivatives

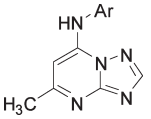

			$IC_{50}(\mu M)$			EC_{50} (μM)
compd	name	Ar	*Pf*DHODH	*Pb*DHODH	*h*DHODH	*Pf* 3D7 cells
1[a]	DSM1	2-naphthyl	0.047	0.23	>200	0.076, 0.066[b]
2[a]	DSM74	4-CF_3-Ph	0.28	0.38	>100	0.34
7	DSM101	4-ethyl-Ph	0.61	3.9	>100	3.3
8	DSM102	4- *n*-propyl-Ph	0.99	9.0	>100	6.8
9	DSM104	4- *n*-butyl-Ph	0.28	5.25	>100	4.8
10	DSM116	4- *n*-pentyl-Ph	0.82	22	>100	>5
11	DSM117	4- *n*-hexyl-Ph	4.2	20	ND	>5
12	DSM118	4- *n*-heptyl-Ph	24	>50	ND	>5
13	DSM119	4- *n*-octyl-Ph	>50	>100	ND	>5
14	DSM103	4-*iso*-propyl-Ph	0.22	0.88	>100	0.78
15	DSM129	4-*tert*-butyl-Ph	0.078	0.4	>100	0.32
16	DSM316	4-*cyclo*-propyl-Ph	0.42	2.9	>100	1.4
17	DSM115	4-venyl-Ph	0.80	4.5	>100	0.34
18	DSM157	4-ethynyl-Ph	1.1	4.1	>100	5.1
19	DSM214	4-CH_2-CF_3-Ph	2.5	8.8	ND	11
20	DSM217	4-S-CF_3-Ph	0.61	1.2	>50	0.27
21	DSM161	4-SF_5-Ph	0.13	0.28	>100	1.3, 0.18[b]
22	DSM156	4- $OCH_2C_6H_5$Ph	5.4	>100	ND	>10
23	DSM130	4-$N(CH_3)_2$-Ph	0.82	12	>100	2.7
24	DSM216	4-pyrrolenyl-Ph	3.5	>50	ND	>20
25	DSM158	4-morpholinyl-Ph	>100	>100	ND	>10
26	DSM229	4-$NHC(CH_3)_3$-Ph	>50	>100	ND	>5
27	DSM248	4-$OC(CH_3)_3$-Ph	44	ND	ND	>10
28	DSM251	4-$C(CH_3)_2CN$-Ph	1.0	ND	ND	3.7
29	DSM228	3-F-4-$C(CH_3)_3$-Ph	0.035	0.11	ND	0.097
30	DSM215	3-F-4-Cl-Ph	0.55	1.3	>50	3.5
31	DSM238	3,4-di-CF_3-Ph	0.54	0.55	>100	2.3
32	DSM190	3,5-di-F-4-CF_3-Ph	0.19	0.28	>30	1.1,0.22[b]
33	DSM159	5,6,7,8-tetrahydro-2-naphthyl	0.064	0.19	>100	0.16
34	DSM160	5-indanyl	0.22	1	>100	0.8
35	DSM127	5-benzodioxolyl	1.6	55	>100	21
36	DSM191	5-benzothiophenyl	0.09	0.6	ND	0.066
37	DSM86	2-CF_3-5-benzo- imidazolyl	21	>50	ND	25

[a] Reported previously.[13,15] ND, not determined. [b] Data were collected in media supplemented with albumax instead of serum. As comparators, data were collected against *Pf* 3D7 cells for chloroquine, pyrimethamine, and atovaquone, EC_{50} = 7.1, 23, and 1.5 nM, respectively, which are similar to reported values.[32−34]

These compounds were all inactive against both *Pf*DHODH and *P. falciparum* 3D7 cells showing that an aromatic ring in this position is important for activity. The addition of a carbon linker between the pendant nitrogen (N1) and the phenyl ring was also explored. The single methyl linker compounds (**54** and **55**) were both inactive, as was **52** containing an oxygen linker. The addition of an ethyl (**56**) or propyl (**57**) linker yielded compounds with midmicromolar range activity against *Pf*DHODH, but these compounds were substantially less active than compounds that do not contain a linker. Compound **58**, containing a simple *n*-heptyl group, showed similar activity to **56** and **57**, consistent with the hydrophobic nature of the binding pocket. This was the only nonaromatic functionality to show activity in this position. In contrast to the inactivity of the straight chain carbon linkers, 2-indanyl (**45**) and derivatives (**46**−**48**) and 1,2,3,4-tetrahydro-2-naphthyl (**49**) and derivatives (**50** and **51**) all showed substantial activity, with most compounds in this series having an IC_{50} against *Pf*DHODH in the 0.5−1.5 μM range. These data suggest that by conformationally restricting the aliphatic linker a favorable interaction with the pocket can be generated even in the absence of a direct conjugation between the pendant nitrogen (N1) and the aromatic ring. The exception is **48**, where the addition of OCH_3 groups onto the 2-indanyl led to reduced activity.

Triazolopyrimidine Ring Modifications. The X-ray structure of **1** and **2** bound to *Pf*DHODH suggested that there is limited

room to increase the size of the triazolopyrimidine ring substituent at positions R and R1 (Figure 2). An exploration of SAR was undertaken to probe the ability of the protein to accommodate additional bulk in these positions, potentially by inducing a conformational change (Table 3). Replacement of the methyl group at R with ethyl (**59**) or CF_3 (**60**) leads to a 2- and 4-fold reduction in *Pf*DHODH inhibitory activity, while in contrast replacement with chloro (**61**) reduced the IC_{50} by 2-fold.

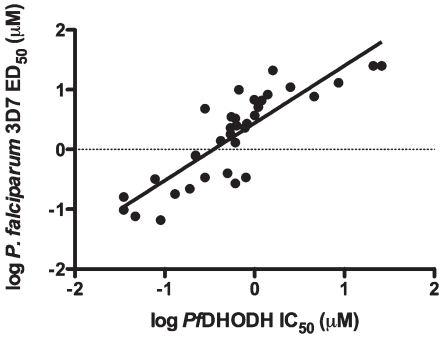

Figure 3. Structure−activity correlation between *Pf*DHODH and *P. falciparum* 3D7 cells. Compounds from Tables 1−3 (using the human serum media) were included in the analysis for those where both enzyme and cell data yielded a determined IC_{50} value. Nonlogarithmic data were fitted by linear regression to determine the parameters of the fit (slope = 0.99; R^2 = 0.67). Data are plotted in log format for clarity of presentation.

Addition of an ethyl to R1 (**62** and **63**) increased the IC_{50} by 3−6-fold over **14**, while the addition of a propyl (**64**) in this position led to complete loss in activity. Finally, cyclyzing the carbon chains of positions R and R1 (**65**) was moderately well tolerated as this compound had an IC_{50} on *Pf*DHODH that was only 2-fold higher than the previously reported analogue with the same aryl group where R = methyl, and R1 = H.[15]

Species Selectivity of Inhibitor Binding. All compounds tested in the series that showed activity against *Pf*DHODH retained good selectivity over the human enzyme, and in no case did we see any activity against human dihydroorotate dehydrogenase (*h*DHODH) (Tables 1−3). However, compounds with good activity against *Pf*DHODH did not always show good activity against *Plasmodium berghei* dihydroorotate dehydrogenase (*Pb*DHODH), showing that significant species variability can occur within the compound series even between the closely related *Plasmodium* species. We previously observed that **1** showed a 5-fold higher IC_{50} for *Pb*DHODH than *Pf*DHODH, while **2** was similarly potent against both enzymes.[15] A similar trend was observed in the extended inhibitor set. Compounds with the most bulky aryl substituents showed the greatest difference in potency, which we interpret as differential binding, between *Pf*DHODH and *Pb*DHODH, with the largest difference (~30-fold) observed for **10** (4-*n*-pentyl-Ph) and **35** (5-benzodioxolyl). Compounds with similar size to **1** showed similar differential binding (~5-fold) between the two enzymes, including **33**, **34**, and **48**−**51**. In contrast, compounds with smaller aryl groups more similar

Table 2. SAR of Alicyclic/Aralkyl and Alkyl Amine-Based Triazolopyrimidine Derivatives

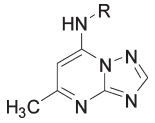

			IC_{50} (μM)			EC_{50} (μM)
compd	name	R	*Pf*DHODH	*Pb*DHODH	*h*DHODH	*Pf* 3D7 cells
38	DSM139	*cyclo*-propyl	>100	ND	ND	ND
39	DSM136	*cyclo*-butyl	>100	ND	ND	ND
40	DSM134	*cyclo*-pentyl	>100	ND	ND	ND
41	DSM135	*cyclo*-hexyl	>100	ND	ND	ND
42	DSM137	*cyclo*-heptyl	>100	ND	ND	ND
43	DSM140	*cyclo*-octyl	>100	ND	ND	ND
44	DSM138	*cyclo*-dodecyl	58	ND	ND	ND
45	DSM162	2-indanyl	0.50	2.4	ND	0.4
46	DSM218	5-F-2-indanyl	0.61	1.4	>50	1.3
47	DSM220	5-Br-2-indanyl	1.2	3.3	>50	6.6
48	DSM219	5,6-di-OCH_3-2-indanyl	4.6	41	ND	7.7
49	DSM192	1,2,3,4-tetrahydro-2-naphthyl	0.54	2.3	ND	1.8
50	DSM236	6-F-1,2,3,4-tetra-hydro-2-naphthyl	0.63	1.9	ND	2.5
51	DSM237	6-Cl-1,2,3,4-tetra-hydro-2-naphthyl	0.67	10	ND	10
52	DSM194	phenyloxy	>100	>100	ND	ND
53[a]	DSM178	benzyl	>100	ND	ND	>10
54[a]	DSM179	4-F-benzyl	>100	ND	ND	>10
55	DSM193	4-CF_3-benzyl	>100	>100	ND	ND
56	DSM213	2-phenylethyl	15	27	ND	>20
57	DSM77	3-phenylpropyl	26	>100	ND	25
58	DSM76	*n*-heptyl	8.6	55	ND	13

[a] Compounds commercially obtained; ND, not determined.

dx.doi.org/10.1021/jm200265b |*J. Med. Chem.* 2011, 54, 3935–3949

Table 3. SAR of Pyrimidine Ring-Modified Triazolopyrimidine Derivatives

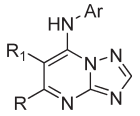

			$IC_{50}(\mu M)$			EC_{50} (μM)
compd	R/R_1	Ar	*Pf*DHODH	*Pb*DHODH	*h*DHODH	*Pf* 3D7 cells
59 (DSM247)	C_2H_5/H	4-CF_3-Ph	0.78	2.0	>100	2.3
60 (DSM235)	CF_3/H	4-CF_3-Ph	1.7	2.3	>100	>10
61 (DSM252)	Cl/H	4-CF_3-Ph	0.17	0.13	>100	3.4
62 (DSM171)[a]	CH_3/C_2H_5	4-$C(CH_3)_2$-Ph	1.7	4.5	>100	>10
63 (DSM172)[a]	CH_3/C_2H_5	4-OCF_3-Ph	3.2	5.7	>100	>10
64 (DSM166)[a]	CH_3/C_3H_7	4-CH_3-Ph	>100	>100	>100	>10
65 (DSM174)[a]	$-C_3H_6-$	3-F-4-CH_3-Ph	1.4	1.3	>100	8.3

[a] Compounds commercially obtained; ND, not determined.

in size to **2** were similarly active against the two enzymes, including **21** and **32**.

In Vitro Absorption, Distribution, Metabolism, and Excretion (ADME) Properties. The goal of identifying triazolopyrimidines with improved potency over **2** was realized for a number of the compounds in Table 1. However, compound potency is only one of the factors important for efficacy in vivo, and thus, select compounds were evaluated to assess their physicochemical properties, protein binding, and in vitro metabolic stability in human and mouse liver microsomes (Table 4). All of the compounds examined had molecular weight (<400), polar surface area (<85 Å^2), number of hydrogen bond donors (<2) and acceptors (≤7), and number of freely rotating bonds (≤5), consistent with the ranges typically targeted for good oral absorption. Log $D_{pH\ 7.4}$ varied from 1.6 to 3.6, and the aqueous solubility at pH 6.5 varied from poorly soluble (**9**, **15**, **20**, **29**, and **32**) to highly soluble (**8**, **16**, **35**, **45**, and **49**). Plasma protein binding, estimated using a rapid chromatographic method calibrated with known protein binding values for reference compounds, was in the range of 87−95% for the majority of compounds.

The most potent compounds, **15**, **29**, **33**, and **36**, all showed CL_{int} values above 30 μL/min/mg microsomal protein, corresponding to predicted hepatic extraction ratios of greater than 0.7 for both mouse and human and suggesting that they would be rapidly metabolized by the liver. The next most potent tier of compounds (**21** and **32**) with IC_{50} values below 0.3 μM and 2−3-fold lower than for **2**, showed more promising results. The CL_{int} values for both **21** and **32** were <6 μL/min/mg protein (corresponding to predicted hepatic extraction ratios of <0.2) in both mouse and human microsomes, suggesting that these compounds will undergo much slower rates of hepatic metabolism in vivo. Compounds **18**, **20**, **45**, and **49** were also predicted to have low in vivo metabolism (CL_{int} values of <10 μL/min/mg protein) in humans; however, they were more rapidly metabolized in mouse liver microsomes (CL_{int} > 25 μL/min/mg protein), suggesting that hepatic clearance could potentially limit systemic exposure of these compounds in the mouse efficacy model. The remaining compounds that were tested all showed high intrinsic clearance values and are therefore likely to undergo significant in vivo hepatic metabolism in both humans and mice.

Mouse Exposure and Pharmacokinetic Analysis in Rats. The systemic exposure of a selection of the more potent compounds was evaluated in mice after a single oral dose of 20 mg/kg, with plasma concentrations measured by LC/MS and followed for 24 h after dosing (Table 5 and Figure 4a). No adverse reactions were observed for any of the compounds after oral administration. Plasma exposure appeared to correlate closely with the in vitro hepatic clearance for most compounds. Compounds **21** and **32**, both of which were stable in mouse liver microsomes, showed significant in vivo exposure with high C_{max} values and prolonged time periods (18 and 19 h, respectively) over which plasma concentrations remained above 1 μM. Interestingly, **32** displayed a high C_{max} and prolonged exposure despite its poor aqueous solubility, suggesting that the permeability of this compound was sufficiently high to overcome the potential solubility limitation. Both compounds displayed a higher C_{max} and more prolonged exposure profiles than compound **2**, based on evaluation of total plasma levels. Compound **49**, which had an intermediate CL_{int} in mouse liver microsomes, had a plasma exposure profile intermediate between the two other groups, although the lower CL_{int} value observed for human liver microsomes suggests that this compound might show relatively better exposure in humans than observed in mice. Compounds with high CL_{int} values (**29**, **14**, **36**, **33**, and **45**) in mouse liver microsomes had poor in vivo exposure, exhibiting a low C_{max} and rapid clearance from the plasma. Compound **29** also had very low aqueous solubility, which may also have contributed to its poor exposure profile. While compounds **29**, **36**, and **33** are significantly more potent than **2**, based on their poor systemic exposure, they would not be expected to show good efficacy in vivo and were therefore not evaluated further.

A more in depth pharmacokinetic analysis of **21** and **32** was performed in rats (Table 6 and Figure 4b) following single IV or oral administration. No adverse reactions were observed for either compound following administration by either dose route. Consistent with the results in mice, both compounds **21** and **32** showed prolonged exposure in rats after oral dosing (20 mg/kg) with a high C_{max} (31 and 34 μM, respectively) and long $T_{1/2}$ (33 and 18 h, respectively). These compounds also had displayed similar binding to rat plasma proteins (95.2 and 97.3% for **21** and **32**, respectively), suggesting that their free concentrations would also be comparable. Oral bioavailability was very high for both compounds; however, an estimated bioavailability of >100% suggests that the pharmacokinetics were dose-dependent over the range of plasma concentrations observed. The IV kinetics of

Table 4. Physicochemical Properties, Plasma Protein Binding, and in Vitro Intrinsic Clearance (CL_{int}) in Liver Microsomes for Selected Triazolopyrimidine Derivatives

compd	Log $D_{pH\ 7.4}$	aqueous solubility pH 6.5 (μM)	human plasma binding (%)[b]	CL_{int} human/mouse (μL/min/mg protein)	E_h human/mouse
1	3.2	45−90	93.8	96/229[a]	0.84/0.91[a]
2	2.5	21−43	86.9	8/ND[a]	0.29/ND[a]
7	2.6	25−50	88.0	61/ND	0.77/ND
8	3.1	187−374	93.5	36/ND	0.66/ND
9	3.6	11−22	96.7	36/ND	0.67/ND
14	3.0	47−94	91.3	30/241	0.64/0.91
15	3.4	11−22	93.2	43/ND	0.71/ND
16	2.7	>377	86.8	53/287	0.75/0.93
17	2.4	25−50	84.4	32/168	0.64/0.88
18	2.2	100−200	81.8	8/27	0.31/0.54
20	3.0	5−10	96.1	<5/119	<0.2/0.84
21	3.0	71−142	95.4	<5/<6	<0.2/<0.2
23	2.2	93−186	ND	9/226	0.4/0.91
29	3.5	<2.7	96.4	32/68	0.64/0.75
32	2.9	9−18	96.6	<5/<6	<0.2/<0.2
33	3.4	89−179	95.5	72/361	0.80/0.94
34	2.9	47−94	92.5	77/341	0.81/0.94
35	1.6	186−372	ND	11/ND	0.37/ND
36	2.6	22−44	89.8	64/162	0.78/0.88
45	2.5	188−376	76.1	<5/32	<0.2/0.59
49	2.9	>358	ND	<5/35	<0.2/0.61

[a] Reported previously.[13,15] ND, not determined. For reference, E_h < 0.3 is indicative of low predicted metabolism, E_h = 0.3−0.6 is medium predicted metabolism, and E_h > 0.7 is high predicted metabolism. [b] Data calculated using the human albumin chromatographic method.

Table 5. Summary of Mouse Exposure Data Following a Single Oral Dose (20 mg/kg)

compd	C_{max} (μM)	time above 1 μM (h)
21	12	19
32	33	18
29	0.25	<1
14	0.8	<1
36	0.4	<1
33	2.2	1
45	0.5	<1
49	7.8	6

both compounds were investigated at two different dose levels. While **21** showed apparently good dose linearity over the 5-fold IV dose range, **32** exhibited clear dose-dependent kinetics over a similar dose range. This dose dependence was not the result of concentration dependent protein binding but rather suggests that the in vivo clearance of **32** is saturable at high dose. It is likely that saturable clearance of **21** is also responsible for the apparent dose dependency with oral administration.

Triazolopyrimidines 21 and 32 Show Good Suppression of *P. berghei* Growth in a Mouse Model. The combined *P. falciparum* whole cell activity data and pharmacokinetic profiles of **21** and **32** in mice suggested that these compounds had the best potential to show good antimalarial activity of the synthesized compounds (Tables 1−3). Both compounds showed a slightly improved potency against *P. falciparum* 3D7 cells when compared to **2** (based on the data collected in albumax), and like **2**, both compounds had similar activity against *Pf*DHODH and *Pb*DHODH, suggesting that they would show activity against *P. berghei*. Both compounds also showed more prolonged exposure profiles when compared with **2**, suggesting that they might show superior efficacy.

Compounds **21** and **32** were assessed using the standard Peter's test[20] in Swiss Webster mice infected with *P. berghei* NK65 ANKA strain. Compounds were dosed orally QD at four dose levels (3, 10, 30, and 100 mg/kg), and parasitemia was assessed 24 h after the last dose to determine the ED_{50} (Figure 5). As a comparator, mice were also dosed with chloroquine (2 mg/kg QD) using the same 4 day dosing protocol. After QD dosing, the ED_{50} was determined to be 17 and 10 mg/kg, respectively, for **21** and **32**. Chloroquine (2 mg/kg) suppressed parasitemia on average by ∼50% (24 h after the last dose) in the two studies, consistent with previous reports that the ED_{50} for chloroquine in this model is ∼2 mg/kg.[20] The effect of BID dosing was also assessed for both **21** and **32**. For **21**, mice treated with either 100 mg/kg QD or 50 mg/kg BID showed low parasitemia levels on day 5 (8 and 2% of controls, respectively, 24 h after the last dose); however, none of the mice were parasite free on any day. In contrast, mice treated with **32** at 100 mg/kg QD or 50 mg/kg BID were parasite free on day 5, with parasitemia reemerging on day 7. Of the mice treated with 100 mg/kg BID, 4/5 remained parasite free through day 7 before parasites reemerged on day 9. Thus, while neither compound was capable of a complete cure, **32** demonstrated superior efficacy to **21**, and both compounds showed better efficacy than **2**, where 50 mg/kg BID dosing was only able to suppress parasitemia by 90% 24 h after the last dose.[15] No adverse reactions were observed that were attributed to drug at any of the dose levels for either compound.

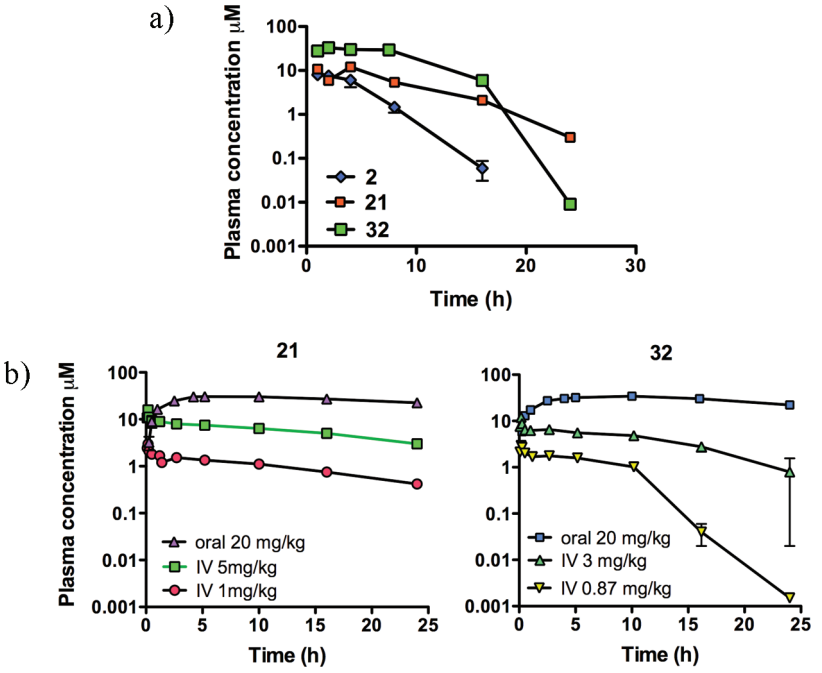

Figure 4. Rodent pharmacokinetic data. (a) Plasma concentration vs time profiles in mice after a single oral dose of 20 mg/kg. Data for **2** were taken from ref 15. (b) Plasma concentration vs time profiles in rats after a single oral or IV dose. Dose and route of dosing are indicated in the figure legend.

Table 6. Rat Pharmacokinetic Parameters for 21 and 32 (Average n = 2 Rats)

parameter	21	32
IV dose (mg/kg)	1, 5.1	0.9, 2.9
clearance (mL/min/kg)[a]	1.5, 1.2	2.3, 1.5
volume of distribution at steady state (L/kg)[a]	1.4, 1.5	0.4, 0.5
$t_{1/2}$ (h)[a]	11.4, 14.5	1.6, 4.5
oral dose (mg/kg)	20.1	18.6
T_{max} (min)	270	600
C_{max} (μM)	31	34.3
$t_{1/2}$ (h)[a]	33	17.6
$AUC_{0\text{-inf}}$ (μM min)[a]	101 693	75 007
bioavailability (F %)[b]	>100	>100

[a] Values are approximations as the terminal elimination phase was not well-defined. [b] Data suggest dose-dependent kinetics.

DISCUSSION

The development of new antimalarial agents is necessary to keep pace with the ongoing evolution of drug resistance and is vital to arm public health efforts against the malaria parasite. The identification of novel chemical agents with antimalarial activity is facilitated by the identification of new targets that provide the opportunity to develop antimalarial drugs from new chemical space.[13,15] Our HTS-based discovery of the triazolopyrimidine-centered *Pf*DHODH inhibitors with antimalarial activity has provided both a new target and a novel lead series for future development. However, to advance the triazolopyrimidine series to clinical development, it was necessary to identify an optimized compound that shows both potency and good pharmacokinetic properties. In pursuit of this objective, we undertook a systematic investigation of replacements/modifications of the aromatic ring systems of compounds **1** and **2**. This effort led to the identification of two compounds, **21** and **32**, with improved in vivo properties over prior analogues in the series, including better efficacy in the mouse *P. berghei* model.

We explored a variety of aryl, alkyl, and alicyclic/aralkyl groups linked to the triazolopyrimidine scaffold through the pendant nitrogen (N1) (Figure 1). As with previous analogs in the series,[13,15] we observed a close correlation between the potency of the compounds as inhibitors of *Pf*DHODH and the activity against *P. falciparum* 3D7 cells. These data provide strong evidence that *Pf*DHODH is the target of cell killing throughout the series. The most potent analogues in the series were naphthyl (**1**, **33**, and **36**) and the 4-*tert*-butyl-phenyl analogues (**15** and **29**). The best of these compounds (**29** and **33**) had IC_{50} values against *Pf*DHODH in the 30 nM range. The next most potent analogues showing midrange IC_{50} values (200−400 nM) contained a hydrocarbon of less than five carbons or a fluorinated species (CF_3 or SF_5) at the *para* position of the aniline ring, with addition of a *meta*-fluorine providing an incremental increase in compound potency. Larger *para* substituents led to reduced activity and most of the other characterized compounds were substantially less potent. Taken together, the data show that the preferred functionality is an aromatic ring system containing 10−12 carbons with two fused rings or an aniline with a bulky hydrophobic group at the *para* position. This observed SAR is consistent with our structural studies, which demonstrate the pocket to be entirely hydrophobic, and on the basis of the X-ray structures of **1** and **2**, little free space remains to accommodate additional groups in the absence of conformational changes in the binding site (Figure 2).

Comparison of the more potent analogues with those that showed poor activity provides additional insight into the nature of the inhibitor binding site. We analyzed an expanded set of heteroatoms in the aryl ring, and these results extend our prior findings that N and O heteroatoms are not tolerated in the aryl group. In contrast, the naphthyl analogue possessing a lipophilic sulfur atom **36** showed good potency, consistent with the highly

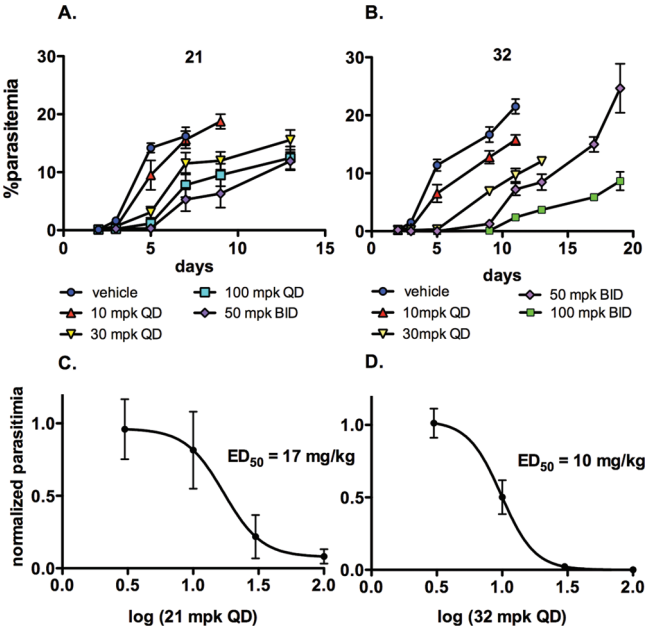

Figure 5. In vivo efficacy of **21** and **32** in the *P. berghei* mouse malarial model. The zero time point represents the day of infection, and once daily oral dosing was performed at 3, 24, 48, and 72 h after infection. Dose levels are indicated on the graphs. Five mice were dosed per group, and error bars represent the standard error of the mean. Percent parasitemia vs time from initial innoculum (days) for **21** (A) and **32** (B). Not all dose levels are shown for clarity of presentation. (C and D) Parasite levels were determined 24 h after the final dose and are plotted as the normalized values (relative to the no drug vehicle control) vs log of drug dose. Data were fitted to the log(inhibitor) vs dose−response variable slope (four parameter) equation in GraphPad Prism to determine the ED_{50}. The ED_{50} = 17 (10−29 mg/kg) and 10 mg/kg (7.6−13 mg/kg), respectively, for **21** and **32**, where the 95% confidence interval is indicated in parentheses.

hydrophobic nature of the aryl binding pocket (Figure 2). We explored the effects of adding either linear alkyl groups or aliphatic ring systems as linkers between the triazolopyrimidine ring and the aryl group. Linear hydrocarbon or heteroalkyl linkers were inactive. However, by utilizing the cycloalkyl ring as the link between the aromatic ring (**49** and **45**) and the pendant nitrogen (N1), activity in the same range as **2** was obtained. These data illustrate that improved potency is obtained by constraining the linker. However, compounds for which the aryl ring was conjugated directly to the pendant nitrogen (N1) (**33** and **34**) were more potent (15- and 2-fold, respectively) than the equivalent analogue where the cycloalkyl ring is instead bound to N1 (**49** and **45**). We previously noted that the pyridine nitrogen (N5) is likely to be electron-rich in character, which facilitates the formation of a H-bond with R265 (Figure 2).[17] These data suggest that the optimal electronics to promote this interaction occur when N1 is coupled directly to an aryl group. Additionally, better π-stacking interactions may be formed with F227 and F188 when the aryl ring is closer to the opening of the hydrophobic pocket (Figure 2). The importance of these interactions is also suggested by the relative inactivity of the alicyclic and alkyl amines and by the inactivity of compounds containing a carbon or oxygen bridge between N1 and the aryl group. Compound **2** (IC_{50} = 0.28 μM) is, for example, significantly more potent than **55** (IC_{50} > 100 μM, benzyl), **56** (IC_{50} = 15 μM, phenethyl), or **57** (IC_{50} = 26 μM, phenpropyl).

All of the tested compounds retain excellent species selectivity showing activity on *Pf*DHODH but not against the human enzyme. Amino acid sequence differences in the aryl pocket likely to account for this selectivity.[17] The activity of the compounds in the series differs between the *P. falciparum* and *P. berghei* DHODH enzymes. The difference is greatest for large aryl or aralkyl groups, while compounds that contain smaller *para* substituents on the aniline show similar binding affinity for both enzymes. Two amino acid differences can be identified in the inhibitor binding pocket between *Pf*DHODH and *Pb*DHODH (G181S and M536 V). The residue at position 536 is in the aryl binding pocket, suggesting that this change is responsible for the observed species differences in binding between the two *Plasmodium* enzymes.

In vitro physicochemical and metabolism studies followed by pharmacokinetic analysis in mice and rats were used to evaluate the likelihood that the compounds would have the in vivo properties required of a drug candidate. The most potent compounds including **29** and **33** were rapidly metabolized in mouse and human microsomes, which is likely the basis for poor plasma exposure after oral dosing in mice; **29** also has very low aqueous solubility at a pH representative of the small intestine, which may have further contributed to its poor oral absorption. While the rapid metabolism prevents **29**, **33**, and **36** from being useful in vivo, all three compounds have similar in vitro activity to **1** and thus should be useful as alternatives to **1** for genetic selection in *P. falciparum* using the yeast DHODH marker that we recently described.[21]

The optimal aryl groups that have the best balance between potency, metabolic stability, and plasma exposure were identified as 4-SF_5-Ph (**21**) and 3,5-di-F-4-CF_3-Ph (**32**). While these compounds were less potent than **29** and **33** against the enzyme, both showed prolonged plasma exposure in the mouse (Table 5) and better efficacy in the *P. berghei* mouse model of malaria when compared with **2**. Compound **32** is the first triazolopyrimidine to be identified that is able to fully clear parasites from the infected mouse, although parasites re-emerged several days later. The EC_{50} values against *P. falciparum* in whole cell assays were ~200 nM for both **21** and **32,** 10−200-fold above the levels for the comparator antimalarial drugs (Table 1). Furthermore, the ED_{50} values against *P. berghei* were 17 and 10 mg/kg, respectively, for **21** and **32**. These values are higher than reported for standard antimalarials (e.g., ED_{50} values for chloroquine, 1.8 mg/kg; mefloquine, 3.8 mg/kg; and artesunate, 5.9 mg/kg),[20,22] possibly explaining why **21** and **32** were not able to fully clear the infection. Regardless, **21** and **32** compare favorably in the Peter's test of *P. berghei* infection to the most potent of the *N*-alkyl-5-(1*H*-benzimidazol-1-yl)thiophene-2-carboxamides *Pf*DHODH inhibitors described by Booker et al., which also were reported to have an ED_{50} of 10−15 mg/kg.[16]

In conclusion, the studies described herein have identified the optimized aryl groups for coupling to the triazolopyrimdine ring that provide the best balance between potency and metabolic stability. Despite the improved properties of **21** and **32**, these compounds likely would benefit from additional optimization to improve potency prior to selection of a drug candidate.

EXPERIMENTAL SECTION

Materials. Compounds **53**, **54**, and **62**−**65** were purchased from ChemDiv. The amine precursors for **31** and **29**, 3,4-bis(trifluoromethyl) aniline and 4-*tert*-butyl-3-fluoroaniline, respectively, were purchased from the

Boston University Chemistry Core (Michael P. Pollastri supervisor). Reagents for enzyme assay and purification were purchased from Sigma unless otherwise noted.

Methods. *Enzyme Purification and Assay.* *Pf*DHODH, *Pb*DHODH, and *h*DHODH were expressed and purified from *Escherichia coli* as His_6-tagged recombinant enzymes as previously described.[13,15,23] All three enzymes were expressed as truncated soluble proteins without the N-terminal membrane spanning domain. DHODH activity was assessed using the 2,6-dichloroindophenol (DCIP) dye-based assay as described[13,15] using final assay conditions as follows: assay buffer (100 mM HEPES, pH 8.0, 150 mM NaCl, 10% glycerol, and 0.1% Triton), substrates (0.2 mM L-dihydroorotate and 0.02 mM CoQ_D), and DCIP (0.12 mM). Reactions were started by the addition of DHODH (E_T = 10 nM) and monitored at 600 nm (ε = 18.8 mM^{-1} cm^{-1}) for 5−10 min at 20 °C. Initial rates were used to determine the reaction velocity in the absence (v_o) and presence (v_i) of inhibitor. Inhibitors were added over a range of 0.01−100 μM using a 3-fold dilution series. Data for each inhibitor concentration were collected in triplicate, and the measured v_i/v_o values were fitted to the log[*I*] vs response (three parameters) equation in Graph Pad Prism to determine the IC_{50}.

P. falciparum Whole Cell Assays. *P. falciparum* 3D7 cells were grown in Gibco-Invitrogen RPMI-1640 supplemented with 2% (w/v) red blood cells and either 20% human type A+ plasma[24] or with Gibco-Invitrogen 0.5% Albumax I. Cultures used in Albumax testing were washed three times in RPMI-1640 to remove plasma-supplemented medium. Cell growth was monitored by [^{3}H]-hypoxanthine uptake as described previously.[25] Data at each concentration point were collected in quadruplicate and were fitted to the log[*I*] vs response−variable slope (four-parameter) model in Graph Pad Prism to determine the concentration of inhibitor that resulted in 50% growth inhibition (ED_{50}).

In Vitro ADME. Partition coefficients ($LogD_{pH\ 7.4}$) were estimated by comparison of their chromatographic retention properties to a series of standard compounds with known values. The method utilized a Waters 2795 HPLC instrument with a Waters 2487 dual channel UV detector and employed a Phenomenex Synergi Hydro-RP 4 μm (30 mm × 2 mm) column and a mobile phase consisting of an aqueous buffer (50 mM ammonium acetate, pH 7.4) and acetonitrile. The acetonitrile content was varied from 0 to 100% over 10 min, and the column was reconditioned prior to the next injection. Compound elution was monitored at 220 and 254 nm.

Protein binding values were estimated by comparison of their chromatographic retention properties on a human albumin column (ChromTech Chiral-HSA 50 mm × 3.0 mm, 5 μm, Sigma-Aldrich) to those of a series of standard compounds with known values. The HPLC system was as above. The mobile phase consisted of an aqueous buffer (25 mM ammonium acetate buffer, pH 7.4) and 30% isopropanol in the same aqueous buffer. Isopropanol composition was varied using a 10 min gradient after which the column was reconditioned prior to the next injection. Compound elution was monitored at 220 and 254 nm.

For **21** and **32**, protein binding in rat plasma was assessed by ultracentrifugation to separate protein bound and free compound. Plasma samples were spiked with compound (200 and 2000 ng/mL) and centrifuged at 37 °C for 4.2 h using a Beckman Optima XL 100K ultracentrifuge (Beckman Rotor type 42.2 Ti; 223000*g*). Supernatant plasma water was assayed for the free compound concentration, and this value was compared to the total concentration in noncentrifuged plasma controls incubated for the same time period at 37 °C to determine the fraction bound.

Nonequilibrium solubility measurements were conducted by dilution of concentrated DMSO stock solutions into pH 6.5 phosphate buffer (final DMSO concentration of 1% v/v) and monitored for precipitate formation using a NEPHELOstar Galaxy Nephelometer (BMG LABTECH GmbH, Offenburg, Germany). The solubility (expressed as a range) was taken to lie within the sample concentration range just prior to detection of a turbidimetric signal above the background reading.

To assess the in vitro metabolic properties compounds (1 μM) were incubated at 37 °C with human and mouse liver microsomes (BD Gentest, Discovery Labware Inc., Woburn, Massachusetts) suspended in 0.1 M phosphate buffer (pH 7.4) at a final protein concentration of 0.4 mg/mL. Metabolic reactions were initiated by the addition of an NADPH-regenerating system (1 mg/mL NADP, 1 mg/mL glucose-6-phosphate, and 1 U/mL glucose-6-phosphate dehydrogenase) and $MgCl_2$ (0.67 mg/mL) and were quenched at various time points up to 60 min by the addition of ice-cold acetonitrile. Control samples lacking the NADPH-regenerating system were included to monitor for noncytochrome P450-mediated metabolism in the microsomal matrix. Quenched samples were centrifuged, and the relative loss of parent compound in the supernatant over the course of the incubation was monitored by LC-MS. Concentration versus time data for each compound were fitted to an exponential decay function to determine the first order rate constant for substrate depletion and the in vitro intrinsic clearance (CL_{int}, μL/min/mg microsomal protein). These values were then used to calculate a predicted in vivo intrinsic clearance value ($CL_{int\ vivo}$) according to the methods of Obach.[26] For simplicity, $CL_{int\ vivo}$ was converted to a predicted in vivo hepatic extraction ratio (E_h) using the following equation: $E_h = CL_{int\ vivo}/Q + CL_{int\ vivo}$, where Q is liver blood flow (20.7 and 90 mL/min/kg in for humans and mice, respectively).[27]

Pharmacokinetic Analysis. Animal studies were performed in accordance with the Australian Code of Practice for the Care and Use of Animals for Scientific Purposes, and the study protocol was approved by the Monash Institute of Pharmaceutical Sciences Animal Ethics Committee.

The systemic exposure of compounds listed in Table 5 was studied following oral administration to nonfasted male Swiss outbred mice. Mice had free access to food and water continuously throughout the pre- and postdose phases of the study. Compounds were administered by oral gavage in an aqueous suspension vehicle (0.5% w/v sodium caboxymethylcellulose, 0.5% v/v benzyl alcohol, and 0.4% v/v Tween 80, 0.1 mL dose volume per mouse). At predefined time points, mice (n = 1 mouse per time point for each compound) were anaesthetized with gaseous isofluorane, and a single blood sample was collected via cardiac puncture. Blood was transferred to heparinized tubes containing a stabilization cocktail (Complete inhibitor cocktail, potassium fluoride, and EDTA) to minimize the potential for ex vivo degradation of test compound. Samples were immediately centrifuged to collect plasma for analysis.

The pharmacokinetics properties of **21** and **32** were also assessed in overnight fasted male Sprague−Dawley rats after IV and oral administration. Rats had access to water ad libitum throughout the pre- and postdose sampling period, and access to food was reinstated 4 h postdose. Compounds were administered intravenously in an aqueous solution vehicle [**21**: 10% DMSO and 1% 1 M HCl in 0.1 M Captisol in water (CyDex Pharmaceuticals Inc., Lenexa, KS); **32**: 10% DMSO, 1% 1 M HCl, and 5% Tween 80 in 5% glucose/0.8% Tween 80 in water] as a 10 min constant rate infusion into the jugular vein at two dose levels (1.0 mL per rat, n = 2 rats per dose level for each compound) and orally by gavage (1.0 mL per rat, n = 2 rats per compound) as an aqueous suspension (**21**: 5% DMSO, 0.5% hydroxypropylmethyl cellulose, 0.5% benzyl alcohol, and 0.4% Tween 80 in water; **32**: 1% DMSO, 0.5% carboxymethyl cellulose, 0.5% benzyl alcohol, and 0.4% Tween 80 in water). After the oral dose was administered, the tube was rinsed with 1 mL of Milli-Q water to collect any residual formulation, and this volume was also administered to the animal. Samples of arterial blood were collected up to 24 h postdose via an in-dwelling carotid cannula. Blood was collected directly into heparinized tubes containing stabilization cocktail as described for the mouse studies and maintained at 4 °C. At the end of the collection period, samples were centrifuged to collect plasma for analysis.

Quantitative analysis of each compound in plasma samples from both the mouse and the rat studies was conducted by LC-MS (on either a

Micromass Quattro Premier or Micromass Xevo TQ) against calibration standards prepared in blank plasma. Both samples and standards were prepared by precipitation with acetonitrile, followed by centrifugation and analysis of the supernatant. The analytical lower limit of quantitation (LLQ) value for each compound in plasma was <0.002 μM for all compounds.

Intravenous and oral pharmacokinetic parameter estimation for **21** and **32** in rats was conducted using noncompartmental methods. WinNonlin software (version 5.2.1, Pharsight Corporation, Mountain View, CA) was utilized for estimation of the terminal elimination half-life ($t_{1/2}$), the area under the plasma concentration versus time profile from time zero to either the last sample time point ($AUC_{0-24\,h}$) or the extrapolated to infinity ($AUC_{0\text{-}inf}$), plasma clearance, and volume of distribution at steady state. The maximum plasma concentration (C_{max}), the time to reach the maximum concentration (T_{max}), and the time plasma concentrations remained above 1 μM ($T_{>1\,\mu M}$) were taken directly from the concentration versus time profiles. The oral bioavailability (%F) for **21** and **32** in rats was estimated by comparing the average dose-normalized $AUC_{0-24\,h}$ (n = 2 rats) after oral administration to the average dose-normalized $AUC_{0-24\,h}$ (n = 2 rats) after IV administration at the higher of the two IV dose levels (i.e., 5 mg/kg for **21** and 3 mg/kg for **32**). Because of the apparent dose dependency in the kinetics, the calculated bioavailability value is an estimate only.

In Vivo P. berghei Efficacy in Mice. The efficacy was assessed using the standard Peter's test as previously described.[20,28] The *P. berghei* NK65 ANKA strain was obtained from MR4 (Malaria Research and Reference Resource Center, Manassas, VA). Eight to ten week old female Swiss Webster mice (20−22 g) were obtained from Charles River (Wilmington, MA). Mice were infected with 2×10^7 infected erythrocytes in 200 μL by intraperitoneal injection. Once a day oral dosing was performed at 3, 24, 48, and 72 h after infection. Test compounds or chloroquine (Sigma-Aldrich, St. Louis, MO) were suspended in the CMC vehicle described above for PK analysis and administered in volumes of 200 μL. Parasitemia was monitored daily starting 24 h postinfection. A minimum of 10 fields (1000× oil immersion) of >100 erythrocytes per field were counted by light microscopy. Animals demonstrating ≥20% loss in preinfected body weight were euthanized in compliance with institutional guidelines. For ED_{50} determination, parasitemia was counted 24 h after the final dose, and data were fitted to the log (inhibitor) versus dose−response variable slope (four parameter) equation in GraphPad Prism to determine the ED_{50}.

Chemistry General Methods. All commercial chemicals and solvents were reagent grade and were used without further purification, unless otherwise specified. Reaction progress was monitored by thin layer chromatography (TLC) using silica gel 60 F-254 (0.25 mm) plates. Visualization was achieved with UV light and iodine vapor. Flash chromatography was carried out with silica gel (32−63 μm). ^{1}H NMR spectra were recorded on dilute solutions in $CDCl_3$ or DMSO-d_6 at 300 MHz. Chemical shifts are reported in parts per million (δ) downfield from tetramethylsilane (TMS). Coupling constants (J) are reported in Hz. Spin multiplicities are described as s (singlet), brs (broad singlet), d (doublet), t (triplet), q (quartet), and m (multiplet). Electrospray ionization mass spectra were acquired on a Bruker Esquire Liquid Chromatograph-Ion Trap Mass Spectrometer. FABHRMS data were obtained on JEOL HX-110 mass spectrometer. Melting points (Pyrex capillary) were determined on a Mel-Temp apparatus and are uncorrected. As a test of purity, compounds were subjected to HPLC analysis on Beckman system gold using a gradient of 20−100% MeOH over 30 min, using a Beckman (ultrasphere) ODS column (5 μ, 4.6 mm × 15 cm). Compounds eluted as a single peak and were judged to be >95% pure.

*General Procedure for Compounds **5a**−**c**.* A mixture of 3-amino-1,2,4-triazole **4** (20 mmol) and appropriate substituted ethyl acetoacetate **3a**−**c** (20 mmol) was heated under reflux in 10 mL of acetic acid for 3.5−8 h. After the reaction mixture cooled to room temperature, the precipitated solid was filtered, washed with acetic acid followed by ethanol, and dried under vacuum and provided the desired products **5a**−**c** with 45−55% yield.

*5-Methyl-[1,2,4]triazolo[1,5-a]pyrimidin-7-ol (**5a**).* mp 287 °C. ^{1}H NMR (300 MHz, DMSO-d_6): δ 8.15 (s, 1H), 5.82 (s, 1H), 2.30 (s, 3H). MS m/z 151.1 $(M + H)^+$.

*5-Ethyl-[1,2,4]triazolo[1,5-a]pyrimidin-7-ol (**5b**).* mp 215 °C. ^{1}H NMR (300 MHz, DMSO-d_6): δ 8.18 (s, 1H), 5.82 (s, 1H), 2.60 (q, 2H), 1.21 (t, 3H). MS m/z 162.9 $(M - H)^+$.

*5-Trifluoromethyl-[1,2,4]triazolo[1,5-a]pyrimidin-7-ol (**5c**).* mp 263 °C. ^{1}H NMR (300 MHz, DMSO-d_6): 8.40 (s, 1H), 8.04 (s, 1H, OH), 6.14 (s, 1H). MS m/z 202.9 $(M - H)^+$.

*[1,2,4]Triazolo[1,5-a]pyrimidin-5,7-diol (**5d**).* To a stirred solution of 4.05 g (59.5 mmol) of NaOEt in 50 mL of absolute EtOH, 9.52 g (59.5 mmol) of ethyl malonate and 9.52 g (59.5 mmol) of 5-amino-[1,2,4]triazole were added, and the mixture was refluxed for 8 h. After it was cooled to room temperature, the precipitated white sodium salt was collected, dissolved in H_2O, and filtered with charcoal, and the filtrate was acidified with concentrated HCl. The resulting precipitate was collected, washed with water, and dried gave 4.5 g (50% yield) of white solid. mp 240 °C (lit 238 °C).[18] ^{1}H NMR (300 MHz, DMSO-d_6): 8.36 (s, 1H), 5.11 (s, 1H).

*General Procedure for Compounds **6a**−**c**.* The proper [1,2,4]triazolo[1,5-*a*]pyrimidin-7-ol **5a**−**c** (10 mmol) was added to 2.75 mL (30 mmol) of phosphorus oxychloride and heated under reflux for 45 min in a round-bottom flask. Excess phosphorus oxychloride was removed by distillation at reduced pressure on a steam bath, and the residue was triturated with ice water. The product was extracted from the aqueous mixture with methylene chloride, evaporated, and purified by column chromatography using 60% EtOAc/hexane. This afforded the products **6a**,**b** with 50−65% yield. Compound **6c** was used for the next step without purification.

*7-Chloro-5-methyl-[1,2,4]triazolo[1,5-a]pyrimidine (**6a**).* mp 150 °C. ^{1}H NMR (300 MHz, $CDCl_3$): δ 8.50 (s, 1H), 7.15 (s, 1H), 2.75 (s, 3H). MS m/z 169.1 $(M + H)^+$.

*7-Chloro-5-ethyl-[1,2,4]triazolo[1,5-a]pyrimidine (**6b**).* mp 184 °C. ^{1}H NMR (300 MHz, DMSO-d_6): δ 8.52 (s, 1H), 7.13 (s, 1H), 3.04 (q, 2H), 1.40 (t, 3H). MS m/z 183.1 $(M + H)^+$.

*5,7-Dichloro-5-methyl-[1,2,4]triazolo[1,5-a]pyrimidine (**6d**).* A mixture of 304 mg (2 mmol) [1,2,4]triazolo[1,5-*a*]pyrimidin-5,7-diol **5d**, 5 mL of $POCl_3$ and 0.25 mL (2 mmol) of *N*,*N*-dimethyl aniline (DMA) were refluxed for 1.5 h, forming a clear solution. The solution was concentrated in a reduced pressure to syrup, which was poured with stirring ice. The aqueous solution was extracted with $CHCl_3$, the extract was washed with H_2O, dried, evaporated, and purified by column chromatography using 20% EtOAc/hexane afforded 257 mg (68% yield) of product **6d**. ^{1}H NMR (300 MHz, $CDCl_3$): δ 8.58 (s, 1H), 7.3 (s, 1H).

*General Procedure for Compounds **7**−**44** and **52**−**61**.* The appropriate amine (1.1 mmol) was added to proper-7-chloro-[1,2,4]triazolo[1,5-*a*]pyrimidine **6a**−**d** (1 mmol) in absolute ethanol (10 mL). The stirring was continued for 2−10 h at room temperature by monitoring with TLC until the starting material **6a**−**d** disappeared. Products were purified by column chromatography with CH_2Cl_2/MeOH/NH_4OH (23:1:1) or EtOAc/hexane. Yields ranged from 50 to 92%.

*N-(4-Ethylphenyl)-5-methyl-[1,2,4]triazolo[1,5-a]pyrimidin-7-amine (**7**)*[29]. mp 174 °C. ^{1}H NMR (300 MHz, DMSO-d_6): δ 10.10 (brs, NH, exchangeable), 8.48 (s, 1H), 7.37−7.29 (m, 4H), 6.32 (s, 1H), 2.68−2.61 (m, 2H), 2.40 (s, 3H), 1.24−1.19 (m, 3H). MS m/z 254.1 $[M + H]^+$.

*N-(4-Propylphenyl)-5-methyl-[1,2,4]triazolo[1,5-a]pyrimidin-7-amine (**8**)*[29]. mp 150 °C. ^{1}H NMR (300 MHz, DMSO-d_6): δ 10.10 (brs, NH, exchangeable), 8.48 (s, 1H), 7.37−7.27 (m, 4H), 6.32 (s, 1H), 2.61−2.56 (m, 2H), 2.40 (s, 3H), 1.68−1.56 (m, 2H), 0.95−0.90 (t, 3H). MS m/z 268.1 $[M + H]^+$.

*N-(4-Butylphenyl)-5-methyl-[1,2,4]triazolo[1,5-a]pyrimidin-7-amine (**9**)*[29]. mp 162 °C. ^{1}H NMR (300 MHz, DMSO-d_6): δ 10.07 (brs, NH, exchangeable), 8.46 (s, 1H), 7.33−7.28 (m, 4H), 6.29 (s, 1H), 2.61−2.58 (m, 2H), 2.42 (s, 3H), 1.58−1.56 (m, 2H), 1.34−1.32 (m, 2H), 0.91−0.89 (t, 3H). MS *m*/*z* 282.2 $[M + H]^+$.

*N-(4-Pentylphenyl)-5-methyl-[1,2,4]triazolo[1,5-a]pyrimidin-7-amine (**10**)*[29]. mp 163 °C. ^{1}H NMR (300 MHz, DMSO-d_6): δ 10.17 (brs, NH, exchangeable), 8.46 (s, 1H), 7.33−7.28 (m, 4H), 6.29 (s, 1H), 2.60−2.58 (m, 2H), 2.43 (s, 3H), 1.78−1.69 (m, 2H), 1.54−1.42 (m, 4H), 1.12−0.89 (m, 3H). MS *m*/*z* 225.3 $[M + H]^+$.

*N-(4-Hexylphenyl)-5-methyl-[1,2,4]triazolo[1,5-a]pyrimidin-7-amine (**11**)*[29]. mp 160 °C. ^{1}H NMR (300 MHz, DMSO-d_6): δ 10.1 (brs, NH exchangeable), 8.48 (s, 1H), 7.35−7.30 (m, 4H), 6.32 (s, 1H), 2.62 (m, 2H), 2.41 (s, 3H), 1.67−1. 53 (m, 2H), 1.38−1.26 (m, 6H), 0.89−0.86 (m, 3H). MS *m*/*z* 310.3 $[M + H]^+$.

*N-(4-Heptylphenyl)-5-methyl-[1,2,4]triazolo[1,5-a]pyrimidin-7-amine (**12**)*[29]. mp 153 °C. ^{1}H NMR (300 MHz, DMSO-d_6): δ 10.2 (brs, NH exchangeable), 8.34 (s, 1H), 7.33−7.36 (m, 4H), 6.28 (s, 1H), 2.7 (m, 2H), 2.39 (s, 3H), 1.6−1.52 (m, 2H), 1.40−1.22 (m, 8H), 0.85 (t, *J* = 6.2 Hz, 3H). MS *m*/*z* 324.4 $[M + H]^+$.

*N-(4-Octylphenyl)-5-methyl-[1,2,4]triazolo[1,5-a]pyrimidin-7-amine (**13**)*[29]. mp 144 °C. ^{1}H NMR (300 MHz, DMSO-d_6): δ 10.1 (brs, NH exchangeable), 8.44 (s, 1H), 7.39−7.36 (m, 4H), 6.29 (s, 1H), 2.70−2.55 (m, 2H), 2.45 (s, 3H), 1.63−1.20 (m, 12H), 0.82 (t, *J* = 6.6 Hz, 3H). MS *m*/*z* 338.3 $[M + H]^+$.

*N-(4-Isopropylphenyl)-5-methyl-[1,2,4]triazolo[1,5-a]pyrimidin-7-amine (**14**)*[29]. mp 185 °C. ^{1}H NMR (300 MHz, DMSO-d_6): δ 10.12 (brs, NH, exchangeable), 8.48 (s, 1H), 7.37−7.27 (m, 4H), 6.32 (s, 1H), 3.20−2.95 (m, 1H), 2.41 (s, 3H), 1.28−1.15 (m, 6H). MS *m*/*z* 268.1 $[M + H]^+$.

*N-(4-tert-Butylphenyl)-5-methyl-[1,2,4]triazolo[1,5-a]pyrimidin-7-amine (**15**)*[29]. mp 237 °C. ^{1}H NMR (300 MHz, DMSO-d_6): δ 10.20 (brs, NH, exchangeable), 8.47 (s, 1H), 7.47 (d, *J* = 8.4 Hz, 2H), 7.35 (d, *J* = 8.1 Hz, 2H), 6.35 (s, 1H), 2.40 (s, 3H), 1.30 (s, 9H). MS *m*/*z* 282.2 $[M + H]^+$.

*N-(4-Cyclopropylphenyl)-5-methyl-[1,2,4]triazolo[1,5-a]pyrimidin-7-amine (**16**)*. mp 159 °C. ^{1}H NMR (300 MHz, $CDCl_3$): δ 10.1 (Brs, 1H, NH-exchangable), 8.47 (S, 1H), 7.29 (m, 4H), 6.28 (S, 1H), 2.48 (s, 3H), 1.94 (m, 1H), 0.97−0.67 (m, 4H) MS *m*/*z* 266.3 $[M + H]^+$.

*N-(4-Vinylphenyl)-5-methyl-[1,2,4]triazolo[1,5-a]pyrimidin-7-amine (**17**)*[29]. mp 180 °C. ^{1}H NMR (300 MHz, CDCl3): δ 8.34 (s, 1H), 8.0 (brs, NH, exchangeable), 7.55−7.52 (m, 2H), 7.36−7.33 (m, 2H), 6.80−6.71 (m, 1H), 6.47 (s, 1H), 5.835−5.776 (d, 1H), 5.362−5.326 (d, 1H), 2.45 (s, 3H). MS *m*/*z* 252.2 $[M + H]^+$.

*N-(4-Ethynylphenyl)-5-methyl-[1,2,4]triazolo[1,5-a]pyrimidin-7-amine (**18**)*. mp 219 °C. ^{1}H NMR (300 MHz, DMSO-d_6): δ 10.25 (brs, NH, exchangeable), 8.01 (s, 1H), 7.55−7.45 (m, 4H), 6.52 (s, 1H), 4.20 (s, 1H), 2.45 (s, 3H), 1.78−1.69 (m, 2H), 1.54−1.42 (m, 4H), 1.12−0.89 (m, 3H). MS *m*/*z* 250.1 $[M + H]^+$.

*N-(4-(2,2,2-trifuoroethyl)phenyl)-5-methyl-[1,2,4]triazolo[1,5-a]pyrimidin-7-amine (**19**)*. mp 204 °C. ^{1}H NMR (300 MHz, DMSO-d_6): δ 10.24 (brs, NH, exchangeable), 8.51 (s, 1H), 7.50−7.43 (m, 4H), 6.44 (s, 1H), 3.76−3.64 (m, 1H), 2.43 (s, 3H). MS *m*/*z* 308.2 $[M + H]^+$.

*5-Methyl-N-(4-(trifuoromethylthio)phenyl)-[1,2,4]triazolo[1,5-a]-pyrimidin-7-amine (**20**)*. mp 236 °C. ^{1}H NMR (300 MHz, DMSO-d_6): δ 10.45 (brs, NH, exchangeable), 8.52 (s, 1H), 7.85−7.79 (m, 2H), 7.65−7.57 (m, 2H), 6.64 (s, 1H), 2.48 (s, 3H). MS *m*/*z* 326.2 $[M + H]^+$.

*N-(4-Pentafluorosulfenylphenyl)-5-methyl-[1,2,4]triazolo[1,5-a]pyrimidin-7-amine (**21**)*[29]. mp 250 °C. ^{1}H NMR (300 MHz, DMSO-d_6): δ 10.51 (brs, NH exchagable), 8.51 (s, 1H), 7.95 (d, *J* = 8.5 Hz, 2H), 7.66 (d, *J* = 7.9 Hz, 2H), 6.74 (s, 1H), 2.45 (s, 3H). MS *m*/*z* 352.2 $[M + H]^+$. FABHRMS calcd for $[C_{12}H_{10}F_5N_5S + H]^+$, 352.06552; determined, 352.06586.

*N-(4-(Benzyloxy)phenyl)-5-methyl-[1,2,4]triazolo[1,5-a]pyrimidin-7-amine (**22**)*[29]. mp 137 °C. ^{1}H NMR (300 MHz, DMSO-d_6): δ 10.05 (brs, NH, exchangeable), 8.55 (s, 1H), 7.55−7.35 (m, 7H), 7.21−7.01 (m, 1H), 6.22 (s, 1H), 5.71 (s, 2H), 2.41 (s, 3H). MS *m*/*z* 332.3 $[M + H]^+$.

*N^1,N^1-Dimethyl-N^4-(5-methyl-[1,2,4]triazolo[1,5-a]pyrimidin-7-yl)-benzene-1,4-diamine (**23**)*[29]. mp 269 °C. ^{1}H NMR (300 MHz, $CDCl_3$): δ 9.89 (brs, NH, exchangeable), 8.45 (s, 1H), 7.22 (d, *J* = 9 Hz, 2H), 6.79 (d, *J* = 7.8 Hz, 2H), 6.08 (s, 1H), 2.93 (s, 6H), 2.36 (s, 3H). MS *m*/*z* 269.1 $[M + H]^+$.

*5-Methyl-N-(4-(pyrrolidin-1-yl)phenyl)-[1,2,4]triazolo[1,5-a]pyrimidin-7-amine (**24**)*[29]. mp 271 °C. ^{1}H NMR (300 MHz, DMSO-d_6): δ 9.86 (brs, NH, exchangeable), 8.45 (s, 1H), 7.20−7.18 (d, 2H), 6.62−6.59 (m, 2H), 6.04 (s, 1H), 3.05−3.25 (m, 4H), 2.36 (s, 3H), 2.01−1.95 (m, 4H). MS *m*/*z* 295.2 $[M + H]^+$.

*N-(4-Morpholinophenyl)-5-methyl-[1,2,4]triazolo[1,5-a]pyrimidin-7-amine (**25**)*[29]. mp 230 °C. ^{1}H NMR (300 MHz, DMSO-d_6): δ 9.95 (brs, NH, exchangeable), 8.48 (s, 1H), 7.35 (d, 2H), 7.05 (d, 2H), 6.22 (s, 1H), 3.76 (m, 4H), 3.15 (m, 4H), 2.40 (s, 3H). MS *m*/*z* 311.2 $[M + H]^+$.

*N^1-tert-Butyl-N^4(5-methyl-[1,2,4]triazolo[1,5-a]pyrimidin-7-yl)benzene-1,4-diamine (**26**)*. ^{1}H NMR (300 MHz, CDCl3): δ 8.38 (s, 1H), 7.72 (brs, NH, exchangeable), 7.15−7.05 (m, 2H), 6.85−6.70 (m, 2H), 6.18 (s, 1H), 2.55 (s, 3H), 1.34 (s, 9H). MS *m*/*z* 297.3 $[M + H]^+$.

*N-(4-tert-Butoxyphenyl)-5-methyl-[1,2,4]triazolo[1,5-a]pyrimidin-7-amine (**27**)*[29]. mp 176 °C. ^{1}H NMR (300 MHz, DMSO-d_6): δ 10.15 (brs, NH, exchangeable), 8.50 (s, 1H), 7.34 (m, 2H), 7.06 (m, 2H), 6.28 (s, 1H), 2.38 (s, 3H), 1.35 (m, 9H). MS *m*/*z* 298.2 $[M + Na]^+$.

*2-Methyl-2-(4-(5-methyl-[1,2,4]triazolo[1,5-a]pyrimidin-7-ylamino)phenyl)propanenitrile (**28**)*. mp 239 °C. ^{1}H NMR (300 MHz, DMSO-d_6): δ 10.3 (brs, NH, exchangeable), 8.5 (s, 1H), 7.7−7.4 (m, 4H), 6.4 (s, 1H), 2.4 (s, 3H), 1.7 (m, 6H). MS *m*/*z* 293.3 $[M + H]^+$.

*N-(4-tert-Butyl-3-fluorophenyl)-5-methyl-[1,2,4]triazolo[1,5-a]pyrimidin-7-amine (**29**)*. mp 276 °C. ^{1}H NMR (300 MHz, CDCl3): δ 10.22 (brs, NH, exchangeable), 8.5 (s, 1H), 7.5−7.2 (m, 3H), 6.5 (s, 1H), 2.5 (s, 3H), 1.35 (s, 9H). MS *m*/*z* 322.4 $[M + Na]^+$.

*N-(4-Chloro-3-fluorophenyl)-5-methyl-[1,2,4]triazolo[1,5-a]pyrimidin-7-amine (**30**)*. mp 285 °C. ^{1}H NMR (300 MHz, DMSO-d_6): δ 10.38 (brs, NH, exchangeable), 8.52 (s, 1H), 7.70−7.65 (m, 1H), 7.58−7.55 (m, 1H), 7.38−7.35 (m, 1H), 6.62 (s, 1H), 2.45 (s, 3H). MS *m*/*z* 278.2 $[M + H]^+$.

*N-(3,4-Bis(trifluoromethyl)phenyl)-5-methyl-[1,2,4]triazolo[1,5-a]pyrimidin-7-amine (**31**)*. ^{1}H NMR (300 MHz, DMSO-d_6): δ 10.75 (brs, NH, exchangeable), 8.55 (s, 1H), 8.13−7.92 (m, 3H), 6.88 (s, 1H).

*N-(3,5-Difluoro-4-(trifluoromethyl)phenyl)-5-methyl-[1,2,4]triazolo[1,5-a]pyrimidin-7-amine (**32**)*. mp 238 °C. ^{1}H NMR (300 MHz, DMSO-d_6): δ 10.76 (brs, NH exchangeable), 8.54 (s, 1H), 7.45 (m, 2H), 6.99 (s, 1H), 2.53 (s, 3H). MS *m*/*z* 330.2 $[M + H]^+$. FABHRMS calcd for $[C_{13}H_8F_5N_5 + H]^+$, 330.07789; determined, 330.07626.

*5-Methyl-N-(5,6,7,8-tetrahydronaphthalen-2yl)-[1,2,4]triazolo-[1,5-a]pyrimidin-7-amine (**33**)*[29]. mp 187 °C. ^{1}H NMR (300 MHz, DMSO-d_6): δ 10.01 (brs, NH, exchangeable), 8.50 (s, 1H), 7.30−7.05 (m, 3H), 6.25 (s, 1H), 2.76−2.65 (m, 2H), 2.48 (s, 3H), 1.96−1.65 (m, 4H). MS *m*/*z* 280.2 $[M + H]^+$.

*N-(2,3-Dihydro1H-inden-5-yl)-5-methyl-[1,2,4]triazolo[1,5-a]pyrimidin-7-amine (**34**)*[29]. mp 228 °C. ^{1}H NMR (300 MHz, DMSO-d_6): δ 10.07 (brs, NH exchangeable), 8.47 (s, 1H), 7.35−7.14 (m, 3H), 6.27 (s, 1H), 2.97−2.80 (m, 4H), 2.39 (s, 3H), 2.13−1.98 (m, 2H). MS *m*/*z* 266.3 $[M + H]^+$.

*N-(Benzo[d][1,3]dioxol-5yl)-5-methyl-[1,2,4]triazolo[1,5-a]pyrimidin-7-amine (**35**)*[29]. mp 241 °C. ^{1}H NMR (300 MHz, DMSO-d_6): δ 10.1 (brs, NH exchangeable), 8.42 (s, 1H), 7.4−7.26 (m, 3H), 6.29 (s, 1H), 5.46 (s, 2H), 2.38 (s, 3H). MS *m*/*z* 270.2 $[M + H]^+$.

*N-(Benzo[b]thiophen-5yl)-5-methyl-[1,2,4]triazolo[1,5-a]pyrimidin-7-amine (**36**)*. mp 244 °C. ^{1}H NMR (300 MHz, DMSO-d_6): δ 10.28 (brs,

NH exchangeable), 8.50 (s, 1H), 8.11 (d, J = 8.2, 1H), 7.95 (s, 1H), 7.87 (d, J = 4.9 Hz, 1H), 7.51 (d, J = 5.4, 1H), 7.45 (d, J = 8.2, 1H), 6.35 (s, 1H), 2.39 (s, 3H). MS m/z 282.3 $[M + H]^+$.

*5-Methyl-N-(2-(trifluoromethyl)-1H-benzo[d]imidazol-5yl)-[1,2,4] triazolo[1,5-a]pyrimidin-7-amine (**37**).* mp 274 °C. ^{1}H NMR (300 MHz, DMSO-d_6): δ 10.3 (brs, NH exchangeable), 8.51 (s, 1H), 7.84−7.74 (m, 2H), 7.47 (d, J = 9 Hz, 1H), 6.35 (s, 1H), 2.38 (s, 3H). MS m/z 334.2 $[M + H]^+$.

*N-Cyclopropyl-5-methyl-[1,2,4]triazolo[1,5-a]pyrimidin-7-amine (**38**).* mp 133 °C. ^{1}H NMR (300 MHz, DMSO-d_6): δ 8.52 (brs, 1H, NH-exchangable), 8.36 (s, 1H), 6.44 (s, 1H), 2.78−2.62 (m, 1H), 2.48 (s, 3H) 0.97−0.67 (m, 4H).

*N-Cyclobutyl-5-methyl-[1,2,4]triazolo[1,5-a]pyrimidin-7-amine (**39**).* mp 103 °C. ^{1}H NMR (300 MHz, DMSO-d_6): δ 8.43 (d, J = 7.16 Hz, 1H, NH-exchangable), 8.38 (s, 1H), 6.26 (s, 1H), 4.27−4.10 (m, 1H), 2.42 (s, 3H), 2.39−2.14 (m, 4H), 1.81−1.63 (m, 2H).

*N-Cyclopentyl-5-methyl-[1,2,4]triazolo[1,5-a]pyrimidin-7-amine (**40**).* ^{1}H NMR (300 MHz, DMSO-d_6): δ 8.37 (s, 1H), 8.04 (d, J = 7.45, 1H, NH exchangalbe), 6.37 (s, 1H), 4.12−3.98 (m, 1H), 2.44 (s, 3H), 2.09−1.52 (m, 8H). MS m/z 302.1 $[M + H]^+$.

*N-Cyclohexyl-5-methyl-[1,2,4]triazolo[1,5-a]pyrimidin-7-amine (**41**).* ^{1}H NMR (300 MHz, DMSO-d_6): δ 8.37 (s, 1H), 7.90 (brs, NH, exchangeable), 6.41 (s, 1H), 3.65−3.49 (m, 1H), 2.43 (s, 3H), 1.97−1.0 (m, 10H).

*N-Cycloheptyl-5-methyl-[1,2,4]triazolo[1,5-a]pyrimidin-7-amine (**42**).* mp 92 °C. ^{1}H NMR (300 MHz, DMSO-d_6): δ 8.37 (s, 1H), 7.89 (d, J = 7.68 Hz, NH exchangable), 6.32 (s, 1H), 3.87−3.66 (m, 1H), 2.44 (s, 3H), 2.0−1.40 (m, 12H).

*N-Cyclooctyl-5-methyl-[1,2,4]triazolo[1,5-a]pyrimidin-7-amine (**43**).* mp 114 °C. ^{1}H NMR (300 MHz, DMSO-d_6): δ 8.37 (s, 1H), 7.9 (d, J = 8.50 Hz), NH, exchangeable), 6.31 (s, 1H), 3.86−3.71 (m, 1H), 2.44 (s, 3H), 1.95−1.44 (m, 14H).

*N-Cyclododecyl-5-methyl-[1,2,4]triazolo[1,5-a]pyrimidin-7-amine (**44**).* mp. 163 °C. ^{1}H NMR (300 MHz, DMSO-d_6): δ 8.36(s, 1H), 7.80 (d, J = 8.5 Hz, NH, exchangeable), 6.27 (s, 1H), 3.83−3.67 (m, 1H), 2.45 (s, 3H), 1.86−1.22 (m, 22H).

*N-(5-Methyl-[1,2,4]triazolo[1,5-a]pyrimidin-7-yl)-O-phenylhydroxylamine (**52**).* mp 143 °C. ^{1}H NMR (300 MHz, DMSO-d_6): δ 9.38 (brs, NH, exchangeable), 8.35 (s, 1H), 7.31−7.15 (m, 3H), 7.05−7.15 (m, 1H), 7.95−6.85 (m, 2H), 2.13 (s, 3H). MS m/z 242.3 $[M + H]^+$.

*5-Methyl-N-(4-trifluoromethyl)benzyl)-[1,2,4]triazolo[1,5-a]pyrimidin-7-amine (**55**).* mp 190 °C. ^{1}H NMR (300 MHz, DMSO-d_6): δ 10.1 (brs, NH exchagable), 8.51 (s, 1H), 7.92 (d, J = 8.2 Hz, 2H), 7.65 (d, J = 7.6 Hz, 2H), 6.79 (s, 1H), 4.41−4.32 (m, 2H), 2.39 (s, 3H). MS m/z 308.2 $[M + H]^+$.

*5-Methyl-N-phenethyl-[1,2,4]triazolo[1,5-a]pyrimidin-7-amine (**56**).* mp 118 °C. ^{1}H NMR (300 MHz, DMSO-d_6): δ 8.36 (s, 1H), 7.27−7.15 (m, 5H), 6.33 (s, 1H), 3.63−3.58 (m, 2H), 2.97−2.92 (m, 2H), 2.41 (s, 3H). MS m/z 254.1 $[M + H]^+$.

*5-Methyl-N-(3-phenyl)propyl)-[1,2,4]triazolo[1,5-a]pyrimidin-7-amine (**57**).* mp 271 °C. ^{1}H NMR (300 MHz, DMSO-d_6): δ 8.38 (s, 1H), 7.32−7.12 (m, 5H), 6.24 (s, 1H), 2.73−2.62 (m, 2H), 2.42 (s, 3H), 2.01−1.90 (m, 2H), 1.69−1.58 (m, 2H). MS m/z 268.1 $[M + H]^+$.

*N-Heptyl-5-methyl-[1,2,4]triazolo[1,5-a]pyrimidin-7-amine (**58**).* mp 75 °C. ^{1}H NMR (300 MHz, DMSO-d_6): δ 8.36 (s, 1H), 6.31 (s, 1H), 2.44 (s, 3H), 1.73−0.66 (m, 15H). MS m/z 248.3 $[M + H]^+$.

*5-Ethyl-N-(4-trifluoromethyl)phenyl-[1,2,4]triazolo[1,5-a]pyrimidin-7-amine (**59**).* mp 222 °C. ^{1}H NMR (300 MHz, DMSO-d_6): δ 10.70 (brs, NH, exchangeable), 8.65 (s, 1H), 7.81−7.69 (m, 4H), 6.75 (s, 1H), 2.74−2.71 (m, 2H), 1.23−1.20 (m, 3H). MS m/z 308.3 $[M + H]^+$.

*5-(Trifluoromethyl)-N-(4-trifluoromethyl)phenyl)-[1,2,4]triazolo[1,5-a]pyrimidin-7-amine (**60**).* mp 211 °C. ^{1}H NMR (300 MHz, CDCl3): δ 8.62 (s, 1H), 8.46 (brs, NH, exchangeable), 7.95−7.85 (m, 2H), 7.58−7.47 (m, 2H), 6.95 (s, 1H). MS m/z 370.4 $[M + Na]^+$.

*5-Chloro-N-(4-trifluoromethyl)phenyl)-[1,2,4]triazolo[1,5-a]pyrimidin-7-amine (**61**)*[29]. mp 224 °C. ^{1}H NMR (300 MHz, $CDCl_3$): δ 8.7 (s, 1H), 7.9−7.7 (m, 4H), 6.6 (s, 1H). MS m/z 314.3 $[M + H]^+$.

*General Procedure for Compounds **45**−**51**.* The appropriate amine (1.1 mmol) was added to 7-chloro-5-methyl-[1,2,4]triazolo[1,5-*a*]pyrimidine **6a** (1 mmol) in 5 mL of DMF, K_2CO_3 (1.2 equiv) stirred under N_2 atmosphere at room temperature for 5−20 h until the compound **6a** disappeared. The crude product was purified by column chromatography using CH_2Cl_2/MeOH/NH_4OH or EtOAc/hexane and resulted in the desired products **45**−**51**. Yields ranged from 70 to 78%.

*N-(2,3-Dihydro-1H-inden-2-yl)-5-methyl-[1,2,4]triazolo[1,5-a]pyrimidin-7-amine (**45**).* mp 192 °C. ^{1}H NMR (300 MHz, $CDCl_3$): δ 8.25 (s, 1H), 7.30−7.24 (m, 4H), 6.14 (brs, NH, exchangeable), 6.13 (s, 1H), 4.38 (m, 1H), 3.56−3.47 (m, 2H), 3.14−3.07 (m, 2H), 2.62 (s, 3H). MS m/z 266.1 $[M + H]^+$.

*N-(5-Fluoro-2,3-dihydro-1H-inden-2-yl)-5-methyl-[1,2,4]triazolo-[1,5-a]pyrimidin-7-amine (**46**).* mp 216 °C. ^{1}H NMR (300 MHz, DMSO-d_6): δ 8.40 (brs, NH, exchangeable), 8.38 (s, 1H), 7.25−7.20 (m, 1H), 7.12−7.05 (m, 1H), 7.04−6.97 (m, 1H), 6.52 (s, 1H), 4.62−4.55 (m, 1H), 3.34−3.32 (m, 2H), 3.12−3.05 (m, 2H), 2.46 (s, 3H). MS m/z 284.2 $[M + H]^+$.

*N-(5-Bromo-2,3-dihydro-1H-inden-2-yl)-5-methyl-[1,2,4]triazolo-[1,5-a]pyrimidin-7-amine (**47**).* mp 164 °C. ^{1}H NMR (300 MHz, $CDCl_3$): δ 8.25 (s, 1H), 7.43 (m, 1H), 7.39−7.36 (m, 1H), 7.17−7.14 (m, 1H), 6.28 (brs, NH, exchangeable), 6.12 (s, 1H), 4.59−4.49 (m, 1H), 3.54−3.42 (m, 2H), 3.22−3.01 (m, 2H), 2.62 (s, 3H). MS m/z 346 $[M + 2]^+$.

*N-(5,6-Dimethoxy-2,3-dihydro-1H-inden-2-yl)-5-methyl-[1,2,4]-triazolo[1,5-a]pyrimidin-7-amine (**48**).* mp 191 °C. ^{1}H NMR (300 MHz, DMSO-d_6): δ 8.38 (s, 1H), 8.36 (brs, NH, exchangeable), 6.88−6.85 (m, 2H), 6.52 (s, 1H), 4.62−4.52 (m, 1H), 3.72 (s, 6H), 3.30−3.20 (m, 2H), 3.12−3.02 (m, 2H), 2.45 (s, 3H). MS m/z 326.3 $[M + H]^+$.

*5-Methyl-N-(1,2,3,4-tetrahydronaphthalen-2-yl)-[1,2,4]triazolo-[1,5-a]pyrimidin-7-amine (**49**).* mp 57 °C. ^{1}H NMR (300 MHz, $CDCl_3$): δ 8.28 (s, 1H), 7.24−7.08 (m, 4H), 6.17 (brs, NH, exchangeable), 6.12 (s, 1H), 4.04 (m, 1H), 3.39−3.25 (m, 1H), 3.08−2.87 (m, 3H), 2.62 (s, 3H), 2.38−2.24 (m, 1H), 2.10−1.92 (m, 1H). MS m/z 280.2 $[M + H]^+$.

*N-(6-Fluoro-1,2,3,4-tetrahydronaphthalen-2-yl)-5-methyl-[1,2,4]-triazolo[1,5-a]pyrimidin-7-amine (**50**).* mp 178 °C. ^{1}H NMR (300 MHz, $CDCl_3$): δ 8.25 (s, 1H), 7.18−7.08 (m, 1H), 6.97−6.78 (m, 2H), 6.17−6.02 (m, 1H and NH, exchangeable), 4.04 (m, 1H), 3.35−3.20 (m, 1H), 3.08−2.78 (m, 3H), 2.55 (s, 3H), 2.26−2.14 (m, 1H), 2.10−1.92 (m, 1H). MS m/z 320.3 $[M + Na]^+$.

*N-(6-Choro-1,2,3,4-tetrahydronaphthalen-2-yl)-5-methyl-[1,2,4]-triazolo[1,5-a]pyrimidin-7-amine (**51**).* ^{1}H NMR (300 MHz, $CDCl_3$): δ 8.28 (s, 1H), 7.25−7.18 (m, 2H), 7.12−7.01 (m, 1H), 6.17−6.12 (m, 1H and NH, exchangeable), 4.08 (m, 1H), 3.30−3.20 (m, 1H), 3.05−2.82 (m, 3H), 2.62 (s, 3H), 2.40−2.30 (m, 1H), 2.15−2.05 (m, 1H). MS m/z 314.3 $[M + H]^+$.

*Procedure for N-tert-Butylbenzene-1,4-diamine (**69**).* A mixture of 1.41 g of 1-fluoro-4-nitrobenzene (**66**) (10 mmol) and 3.15 mL of the *tert*-butyl amine (30 mmol) in DMSO (20 mL) was placed in a RB flask and heated at 50 °C for 96 h. After the completion of the reaction, the mixture was poured on to crushed ice and extracted with EtOAc. The organic layer was dried, evaporated, and purified by column chromatography (2% EtOAc/Hex) and gave 1.5 g (77% yield) of *N-tert*-butyl-4-nitroaniline (**67**).[30] ^{1}H NMR (300 MHz, $CDCl_3$): δ 8.03 (d, J = 9 Hz, 2H), 6.55 (d, J = 8.9 Hz, 2H), 4.64 (brs, NH, exchangeable), 1.43 (s, 9H).

N-tert-Butyl-4-nitroaniline (**67**) (194 mg, 1 mmol) was dissolved in 10 mL of MeOH, added to 20 mg of 10% Pd−C, and hydrogenated at room temperature for 3 h. The reaction completion was monitored by TLC and filtered through Celite. The filtrate (**69**) was evaporated and used for the next step without further purification. ^{1}H NMR (300 MHz,

$CDCl_3$): δ 6.95 (d, *J* = 8.9 Hz, 2H), 6.81 (d, *J* = 8.8 Hz, 2H), 3.72 (brs, NH, exchangeable), 1.41 (s, 9H).

*Procedure for N-tert-Butoxyaniline (**70**).* To the stirred solution of potassium *tert*-butoxide 795 mg (7.1 mmol) in 10 mL of DMF under N_2 was added 0.75 mL of 1-fluoro-4-nitrobenzene (**66**) (7.1 mmol), and stirring was continued for 2 h at room temperature. The reaction was quenched with ice cold water, extracted with EtOAc, dried, evaporated, and purified (2% EtOAc/Hex) and gave 656 mg (56% yield) of 1-*tert*-butoxy-4-nitroaniline (**68**).[31] ^{1}H NMR (300 MHz, $CDCl_3$): δ 8.20 (m, 2H), 7.02 (m, 2H), 1.50 (s, 9H).

1-*tert*-Butoxy-4-nitroaniline (**68**) (150 mg, 0.769 mmol) was dissolved in the 10 mL of MeOH, 20 mg of 10% Pd−C was added, and it was hydrogenated at room temperature overnight. The reaction completion was monitored by TLC and filtered through Celite. The filtrate (**70**) was evaporated and used for the next step without further purification. ^{1}H NMR (300 MHz, $CDCl_3$): δ 6.90 (m, 2H), 6.70 (m, 2H), 3.50 (brs, NH, exchangeable), 1.21 (s, 9H).

AUTHOR INFORMATION

Corresponding Author

*Tel: 214-645-6164. E-mail: margaret.phillips@UTSouthwestern.edu (M.A.P.). Tel: 206-221-6069. E-mail: rathod@chem.washington.edu (P.K.R.).

Funding Sources

This work was supported by the United States National Institutes of Health Grants, U01AI075594 (to M.A.P., P.K.R., S.A.C., and I.B.; Malaria Medicines Venture). M.A.P. also acknowledges the support of the Welch Foundation (I-1257), and P.K.R. also acknowledges support from NIH Grants AI089688, AI082617, and the Grand Challenge Explorations Award from the Bill and Melinda Gates Foundation. M.A.P. holds the Carolyn R. Bacon Professorship in Medical Science and Education.

ABBREVIATIONS USED

*Pf*DHODH, *Plasmodium falciparum* dihydroorotate dehydrogenase; *Pb*DHODH, *Plasmodium berghei* dihydroorotate dehydrogenase; *h*DHODH, human dihydroorotate dehydrogenase; CoQ, ubiquinone/coenzyme Q; FMN, flavin mononucleotide; HTS, high-throughput screen; ACTs, artemisinin-based combination therapies; NADH, nicotinamide adenine dinucleotide; ADME, absorption, distribution, metabolism and excretion

REFERENCES

(1) Greenwood, B. M.; Fidock, D. A.; Kyle, D. E.; Kappe, S. H.; Alonso, P. L.; Collins, F. H.; Duffy, P. E. Malaria: Progress, perils, and prospects for eradication. *J. Clin. Invest.* **2008**, *118*, 1266–1276.

(2) Feachem, R. G.; Phillips, A. A.; Hwang, J.; Cotter, C.; Wielgosz, B.; Greenwood, B. M.; Sabot, O.; Rodriguez, M. H.; Abeyasinghe, R. R.; Ghebreyesus, T. A.; Snow, R. W. Shrinking the malaria map: Progress and prospects. *Lancet* **2010**, *376*, 1566–1578.

(3) Eastman, R. T.; Fidock, D. A. Artemisinin-based combination therapies: A vital tool in efforts to eliminate malaria. *Nat. Rev. Microbiol.* **2009**, *7*, 864–874.

(4) White, N. J. Antimalarial drug resistance. *J. Clin. Invest.* **2004**, *113*, 1084–1092.

(5) Mackinnon, M. J.; Marsh, K. The selection landscape of malaria parasites. *Science* **2010**, *328*, 866–871.

(6) Dondorp, A. M.; Yeung, S.; White, L.; Nguon, C.; Day, N. P.; Socheat, D.; von Seidlein, L. Artemisinin resistance: Current status and scenarios for containment. *Nat. Rev. Microbiol.* **2010**, *8*, 272–280.

(7) Dondorp, A. M.; Nosten, F.; Yi, P.; Das, D.; Phyo, A. P.; Tarning, J.; Lwin, K. M.; Ariey, F.; Hanpithakpong, W.; Lee, S. J.; Ringwald, P.; Silamut, K.; Imwong, M.; Chotivanich, K.; Lim, P.; Herdman, T.; An, S. S.; Yeung, S.; Singhasivanon, P.; Day, N. P.; Lindegardh, N.; Socheat, D.; White, N. J. Artemisinin resistance in *Plasmodium falciparum* malaria. *N. Engl. J. Med.* **2009**, *361*, 455–467.

(8) Wells, T. N.; Alonso, P. L.; Gutteridge, W. E. New medicines to improve control and contribute to the eradication of malaria. *Nat. Rev. Drug Discovery* **2009**, *8*, 879–891.

(9) Olliaro, P.; Wells, T. N. The global portfolio of new antimalarial medicines under development. *Clin. Pharmacol. Ther.* **2009**, *85*, 584–595.

(10) Vaidya, A. B.; Mather, M. W. Mitochondrial Evolution and Functions in Malaria Parasites. *Annu. Rev. Microbiol.* **2009**, *63*, 249–267.

(11) Phillips, M. A.; Rathod, P. K. Plasmodium dihydroorotate dehydrogenase: a promising target for novel anti-malarial chemotherapy. *Infect. Disord.: Drug Targets* **2010**, *10*, 226–239.

(12) Baldwin, J.; Michnoff, C. H.; Malmquist, N. A.; White, J.; Roth, M. G.; Rathod, P. K.; Phillips, M. A. High-throughput screening for potent and selective inhibitors of *Plasmodium falciparum* dihydroorotate dehydrogenase. *J. Biol. Chem.* **2005**, *280*, 21847–21853.

(13) Phillips, M. A.; Gujjar, R.; Malmquist, N. A.; White, J.; El Mazouni, F.; Baldwin, J.; Rathod, P. K. Triazolopyrimidine-based dihydroorotate dehydrogenase inhibitors with potent and selective activity against the malaria parasite, *Plasmodium falciparum*. *J. Med. Chem.* **2008**, *51*, 3649–3653.

(14) Patel, V.; Booker, M.; Kramer, M.; Ross, L.; Celatka, C. A.; Kennedy, L. M.; Dvorin, J. D.; Duraisingh, M. T.; Sliz, P.; Wirth, D. F.; Clardy, J. Identification and characterization of small molecule inhibitors of *Plasmodium falciparum* dihydroorotate dehydrogenase. *J. Biol. Chem.* **2008**, *283*, 35078–35085.

(15) Gujjar, R.; Marwaha, A.; El Mazouni, F.; White, J.; White, K. L.; Creason, S.; Shackleford, D. M.; Baldwin, J.; Charman, W. N.; Buckner, F. S.; Charman, S.; Rathod, P. K.; Phillips, M. A. Identification of a metabolically stable triazolopyrimidine-based dihydroorotate dehydrogenase inhibitor with antimalarial activity in mice. *J. Med. Chem.* **2009**, *52*, 1864–1872.

(16) Booker, M. L.; Bastos, C. M.; Kramer, M. L.; Barker, R. H., Jr.; Skerlj, R.; Bir Sdhu, A.; Deng, X.; Celatka, C.; Cortese, J. F.; Guerrero Bravo, J. E.; Krespo Llado, K. N.; Serrano, A. E.; Angulo-Barturen, I.; Belén Jiménez-Díaz, M.; Viera, S.; Garuti, H.; Wittlin, S.; Papastogiannidis, P.; Lin, J.; Janse, C. J.; Khan, S. M.; Duraisingh, M.; Coleman, B.; Goldsmith, E. J.; Phillips, M. A.; Munoz, B.; Wirth, D. F.; Klinger, J. D.; Wiegand, R.; Sybertz, E. Novel inhibitors of *Plasmodium falciparum* dihydroorotate dehydrogenase with anti-malarial activity in the mouse model. *J. Biol. Chem.* **2010**, *285*, 33054–33064.

(17) Deng, X.; Gujjar, R.; El Mazouni, F.; Kaminsky, W.; Malmquist, N. A.; Goldsmith, E. J.; Rathod, P. K.; Phillips, M. A. Structural plasticity of malaria dihydroorotate dehydrogenase allows selective binding of diverse chemical scaffolds. *J. Biol. Chem.* **2009**, *284*, 26999–27009.

(18) Makisumi, Y. Synthesis of potential anticancer agents. 5,7-Disubstituted s-triazolo[2,3-a]pyrimidines. *Chem. Pharm. Bull.* **1961**, *9*, 801.

(19) Guiguemde, W. A.; Shelat, A. A.; Bouck, D.; Duffy, S.; Crowther, G. J.; Davis, P. H.; Smithson, D. C.; Connelly, M.; Clark, J.; Zhu, F.; Jimenez-Diaz, M. B.; Martinez, M. S.; Wilson, E. B.; Tripathi, A. K.; Gut, J.; Sharlow, E. R.; Bathurst, I.; El Mazouni, F.; Fowble, J. W.; Forquer, I.; McGinley, P. L.; Castro, S.; Angulo-Barturen, I.; Ferrer, S.; Rosenthal, P. J.; Derisi, J. L.; Sullivan, D. J.; Lazo, J. S.; Roos, D. S.; Riscoe, M. K.; Phillips, M. A.; Rathod, P. K.; Van Voorhis, W. C.; Avery, V. M.; Guy, R. K. Chemical genetics of *Plasmodium falciparum*. *Nature* **2010**, *465*, 311–315.

(20) Fidock, D. A.; Rosenthal, P. J.; Croft, S. L.; Brun, R.; Nwaka, S. Antimalarial drug discovery: Efficacy models for compound screening. *Nat. Rev. Drug Discovery* **2004**, *3*, 509–520.

(21) Ganesan, S. M.; Morrisey, J. M.; Ke, H.; Painter, H. J.; Laroiya, K.; Phillips, M. A.; Rathod, P. K.; Mather, M. W.; Vaidya, A. B. Yeast dihydroorotate dehydrogenase as a new selectable marker for *Plasmodium falciparum* transfection. *Mol. Biochem. Parasitol.* **2011**, *177*, 29–34.

(22) Nzila, A.; Rottmann, M.; Chitnumsub, P.; Kiara, S. M.; Kamchonwongpaisan, S.; Maneeruttanarungroj, C.; Taweechai, S.; Yeung, B. K.;

Goh, A.; Lakshminarayana, S. B.; Zou, B.; Wong, J.; Ma, N. L.; Weaver, M.; Keller, T. H.; Dartois, V.; Wittlin, S.; Brun, R.; Yuthavong, Y.; Diagana, T. T. Preclinical evaluation of the antifolate QN254, 5-chloro- N′6′-(2,5-dimethoxy-benzyl)-quinazoline-2,4,6-triamine, as an antimalarial drug candidate. *Antimicrob. Agents Chemother.* **2010**, *54*, 2603–2610.

(23) Baldwin, J.; Farajallah, A. M.; Malmquist, N. A.; Rathod, P. K.; Phillips, M. A. Malarial dihydroorotate dehydrogenase: Substrate and inhibitor specificity. *J. Biol. Chem.* **2002**, *277*, 41827–41834.

(24) Desjardins, R. E.; Canfield, C. J.; Haynes, J. D.; Chulay, J. D. Quantitative assessment of antimalarial activity in vitro by a semiautomated microdilution technique. *Antimicrob. Agents Chemother.* **1979**, *16*, 710–718.

(25) Jiang, L.; Lee, P.; White, J.; Rathod, P. Potent and selective activity of a combination of thymidine and 1843U89, a folate-based thymidylate synthase inhibitor, against *Plasmodium falciparum*. *Antimicrob. Agents Chemother.* **2000**, *44*, 1047–1050.

(26) Obach, R. S. Prediction of human clearance of twenty-nine drugs from hepatic microsomal intrinsic clearance data: An examination of in vitro half-life approach and nonspecific binding to microsomes. *Drug Metab. Dispos.* **1999**, *27*, 1350–1359.

(27) Davies, B.; Morris, T. Physiological parameters in laboratory animals and humans. *Pharm. Res.* **1993**, *10*, 1093–1095.

(28) Dominguez, J. N.; Leon, C.; Rodrigues, J.; Gamboa de Dominguez, N.; Gut, J.; Rosenthal, P. J. Synthesis of chlorovinyl sulfones as structural analogs of chalcones and their antiplasmodial activities. *Eur. J. Med. Chem.* **2009**, *44*, 1457–1462.

(29) Phillips, M. A.; Rathod, P. K.; Gujjar, R.; Marwaha, A. S.; Charman, S. A. Dihydroorotate dehydrogenase inhibitors with selective anti-malarial activity. WO Patent 2009/082691; U.S. Patent 20090209557, 2009.

(30) Kotsuki, H.; Kobayashi, S.; Matsumoto, K.; Suenaga, H.; Nishizawa, H. A convenient synthesis of aromatic amines from activated aromatic fluorides. Synthesis. *Synthesis* **1990**, 1147–1148.

(31) Woiwode, T. F.; Rose, C.; Wandless, T. J. A simple and efficient method for the preparation of hindered alkyl-aryl ethers. *J. Org. Chem.* **1998**, *63*, 9594–9596.

(32) Sidhu, A. B.; Verdier-Pinard, D.; Fidock, D. A. Chloroquine resistance in *Plasmodium falciparum* malaria parasites conferred by pfcrt mutations. *Science* **2002**, *298*, 210–213.

(33) Yuvaniyama, J.; Chitnumsub, P.; Kamchonwongpaisan, S.; Vanichtanankul, J.; Sirawaraporn, W.; Taylor, P.; Walkinshaw, M. D.; Yuthavong, Y. Insights into antifolate resistance from malarial DHFR-TS structures. *Nat. Struct. Biol.* **2003**, *10*, 357–365.

(34) Khositnithikul, R.; Tan-Ariya, P.; Mungthin, M. In vitro atovaquone/proguanil susceptibility and characterization of the cytochrome b gene of *Plasmodium falciparum* from different endemic regions of Thailand. *Malar. J.* **2008**, *7*, 23.